

NASA  
Contractor Report 191047

9916  
Army Research Laboratory  
Contractor Report ARL-CR-13  
54P

# Hot Gas Ingestion Effects on Fuel Control Surge Recovery and AH-1 Rotor Drive Train Torque Spikes

Frank Tokarski, Mihir Desai, Martin Books, and Raymond Zagranski  
*Coltec Industries*  
*West Hartford, Connecticut*

April 1994

(NASA-CR-191047) HOT GAS INGESTION  
EFFECTS ON FUEL CONTROL SURGE  
RECOVERY AND AH-1 ROTOR DRIVE TRAIN  
TORQUE SPIKES Final Report, Sep. -  
Oct. 1992 (Coltec Industries)  
54 p

N94-34993

Unclas

G3/07 0009916

Prepared for  
Lewis Research Center  
Under Contract NAS3-26075



National Aeronautics and  
Space Administration





## ABSTRACT

This report summarizes the work accomplished through computer simulation to understand the impact of the hydromechanical turbine assembly (TA) fuel control on rocket gas ingestion induced engine surges on the AH-1 (Cobra) helicopter. These surges excite the lightly damped torsional modes of the Cobra rotor drive train and can cause overtorquing of the tail rotor shaft.

The simulation studies show that the hydromechanical TA control has a negligible effect on drive train resonances because its response is sufficiently attenuated at the resonant frequencies. However, a digital electronic control working through the TA control's separate, emergency fuel metering system has been identified as a solution to the overtorquing problem. State-of-the-art software within the electronic control can provide active damping of the rotor drive train to eliminate excessive torque spikes due to any disturbances including engine surges and aggressive helicopter maneuvers.

Modifications to the existing TA hydromechanical control are relatively minor, and existing engine sensors can be utilized by the electronic control. Therefore, it is concluded that the combination of full authority digital electronic control (FADEC), with hydromechanical backup using the existing TA control enhances flight safety, improves helicopter performance, reduces pilot workload. . .and provides a substantial payback for very little investment.

## PREFACE

This is the final report covering work completed under Contract NAS3-26075 during the period September, 1992 to October, 1992.

The program was conducted under the technical direction of Messrs. George Bobula, U.S. Army Propulsion Directorate and Mike McCall, U.S. Army Aviation Systems Command, for the NASA Lewis Research Center, Cleveland, Ohio. The work was performed by Coltec Industries, Chandler Evans Control Systems Division. Mr. Ray Zagranski was Program Manager and Frank Tokarski, Mihir Desai, and Martin Books were the principal engineers.

## TABLE OF CONTENTS

SUMMARY .....	1
INTRODUCTION .....	2
SIMULATION MODEL .....	3
Fuel Control .....	3
Engine .....	7
Rotor Drive Train .....	10
Airframe .....	10
DISCUSSION OF RESULTS .....	16
Simulation of Rocket Fire Surges .....	16
Potential Solution Using the Existing TA Hydromechanical Control .....	21
Active Damping via Electronic Control .....	25
Performance Benefits .....	31
PRELIMINARY DESIGN...FADEC SYSTEM .....	35
Electronic Control Unit .....	35
TA Control Modifications .....	39
Engine and Airvehicle Modifications .....	41
CONCLUSIONS AND RECOMMENDATIONS .....	43
APPENDIX A .....	
List of Symbols and Acronyms .....	46
List of Figures .....	48



## SUMMARY

A non-linear computer simulation of the Chandler Evans TA hydromechanical fuel control, Lycoming T53 engine, and Bell Helicopter AH-1 Cobra airvehicle was configured on a 386 based PC. This simulation is capable of modeling the engine and helicopter throughout its operating range from engine startup to maximum power and from sea level to 20,000 ft. altitude.

MK66 rocket firings were simulated by disturbing the engine inlet conditions with pressure (P1) and temperature (T1) pulses representative of hot gas ingestions. These pulses were applied as single shots and as multiple firings at the two pilot selectable frequencies (6.3 Hz and 8.3 Hz).

It was shown that the hydromechanical fuel control filtered out the high frequency P1 and T1 disturbances from its metered fuel flow and compressor geometry control outputs. Therefore, the dominant effect to the helicopter was determined to be the repeated engine surges that occur during multiple rocket firings. These result in torque disturbances to the rotor drive train at frequencies very near the tail rotor resonant mode (7.3 Hz). Under these conditions, the lightly damped rotor drive train resonates beyond the normal operating torque limits of the tail rotor shaft.

Methods of reducing engine power via fuel flow and engine geometry in an attempt to lower the nominal value of drive train torque and thus the peak torque oscillation were unsuccessful. The simulation revealed that these potentially corrective inputs needed to be applied very rapidly and that these inputs acted as additional disturbances to the rotor drive train. Therefore, larger resonant torque spikes were caused as compared to doing nothing.

A solution to this dilemma was found to be the incorporation of "active damping" of the rotor drive train resonances via the fast combustive torque response of the engine. Combustive torque is that thermodynamic component of engine output torque that is achieved via additional engine burn flow at a constant gas generator speed. Since the gas generator does not have to change speed, combustive torque response is fast. Active damping applies combustive torque in direct opposition to drive train oscillations in order to reduce their magnitude.

An electronic control with multivariable control algorithms specifically sized to damp the rotor drive train resonances via the engine's combustive torque was simulated and found to keep tail rotor drive shaft torque spikes within normal operating limits. This performance was achieved during single as well as multiple rocket firings. This controller also provides an inherently faster engine and rotor speed control loop for normal operation. Thus, transient rotor speed droop and engine torque overshoots during aggressive maneuvers are significantly reduced compared to the existing bill-of-material control. Thus, a side benefit is increased helicopter agility with less pilot workload.

A preliminary design of the electronic controller was made. An airframe mounted full authority digital electronic control (FADEC) communicating via a small electric motor interface to the existing TA hydromechanical control was the most straight forward and cost effective installation. The electric motor rotates the separate emergency fuel valve in the TA control while the primary hydromechanical control remains operational with its fuel valve not in control of engine fuel flow. If failure of the electronic control should occur, fuel flow remains fixed and the pilot can transfer to the primary hydromechanical control. Thus, the state-of-the-art electronic control is backed up by the existing TA control. Flight safety is improved as well as helicopter performance.

The estimated cost of adding the FADEC and making modifications to the TA hydromechanical assembly is equal to approximately the cost of overhauling the existing TA control. Thus a substantial payback in helicopter safety and performance can be realized for very little investment.

## INTRODUCTION

The AH-1 Cobra helicopter has the capability to launch 2.75 inch folding fin aerial rockets (FFARs) equipped with Mark 66 (MK66) rocket motors to engage battlefield targets. Following a class A accident in which an AH-1 suffered a tail rotor drive shaft failure while launching MK66 FFARs, a joint engineering investigation of the AH-1F helicopter was conducted by the Airworthiness Qualification Test Directorate (RQTD) of the U.S. Army Aviation Technical Test Center and the U.S. Army Aviation Applied Technology Directorate (AATD). The results of this investigation which recommend an engine inlet shield to deflect rocket exhaust gases away from the engine are contained in a U.S. Army Test and Evaluation Command (TECOM) Final Report, TECOM Project No. 4-CO-230-000-016, dated June 1991.

Subsequent to this work, the U.S. Army Aviation Systems Command (AVSCOM) in conjunction with the NASA Lewis Research Center directed Chandler Evans, the engine fuel control supplier for the AH-1 helicopter, to investigate potential modifications to the fuel control to alleviate the rocket fire surge problem. The work at Chandler Evans was based on a computer simulation of the engine, fuel control, and AH-1 helicopter.

The objective of the investigation was not to preclude engine surge following hot gas ingestion but to recover smoothly from surge and avoid overtorquing the rotor drive system. This objective, if achieved, would have application not only to rocket firings, but to helicopter operation in general where inlet distortion effects and engine deterioration can also cause the engine to surge and potentially cause damage to the rotor drive train.



## SIMULATION MODEL

The simulation model is a non-linear representation of the complete AH-1/T53 engine control system as illustrated in Figure 1. The 1500 SHP, T53-L-703 turboshaft engine is coupled to the Bell Helicopter AH-1F Cobra Gunship's rotor drive train. The Chandler Evans TA-7 hydromechanical control is interfaced to the Cobra cockpit and controls engine power in response to pilot commands. Rotor speed governing as well as engine overfueling, surge, and blowout protection are provided by the TA control. Details of the complete engine, control and airframe models are included below.

### **Fuel Control**

The Chandler Evans TA control is a full authority hydromechanical assembly that schedules engine fuel flow, compressor inlet guide vane position, and interstage bleed band position for safe engine operation throughout its operating envelope.

A simplified functional block diagram of the TA hydromechanical computer is illustrated in Figure 2. The control law is based on  $Wf/\delta$ , where  $\delta = P1/14.7$ . Therefore, the proportional power turbine and gas generator speed governors both modulate  $Wf/\delta$ . The governor requesting the lowest  $Wf/\delta$  is in control of the engine.

Typically, the pilot sets the gas generator governor's PLA to maximum. This provides a maximum power available setting to protect the engine against overspeeds and overtorques. The collective pitch stick in the cockpit is then modulated to fly the helicopter. This stick is mechanically coupled to the power turbine governor lever which schedules low  $Wf/\delta$  for low collective pitch settings (low power) and high  $Wf/\delta$  for high collective pitch settings (high power). This arrangement essentially schedules, on an open loop basis, the engine power needed to keep the helicopter rotor speed constant at various load requirements (i.e., collective pitch settings).

However, due to varying flight conditions such as airspeed, climb and descent rate, rapid collective pitch pulls/chops, etc. the aerodynamic rotor loads vary and tend to change rotor speed. The proportional power governor turbine senses these changes and automatically compensates  $Wf/\delta$  (and thus engine power) to minimize rotor speed changes. Furthermore, the pilot has the ability to trim out rotor speed errors during steady flight conditions by utilizing the beeper motor to adjust  $Wf/\delta$ .

The acceleration and deceleration schedules are functions of N1 and T1 and provide top and bottom  $Wf/\delta$  limits to preclude engine surge and flameout during rapid engine power transitions.

As shown in Figure 2, the winning  $Wf/\delta$  is mechanically multiplied by  $\delta$ . The P1 input provides altitude compensation by reducing fuel flow and governor gains at high altitude where low fuel flow is required to match the reduced engine airflow and to maintain closed loop stability.

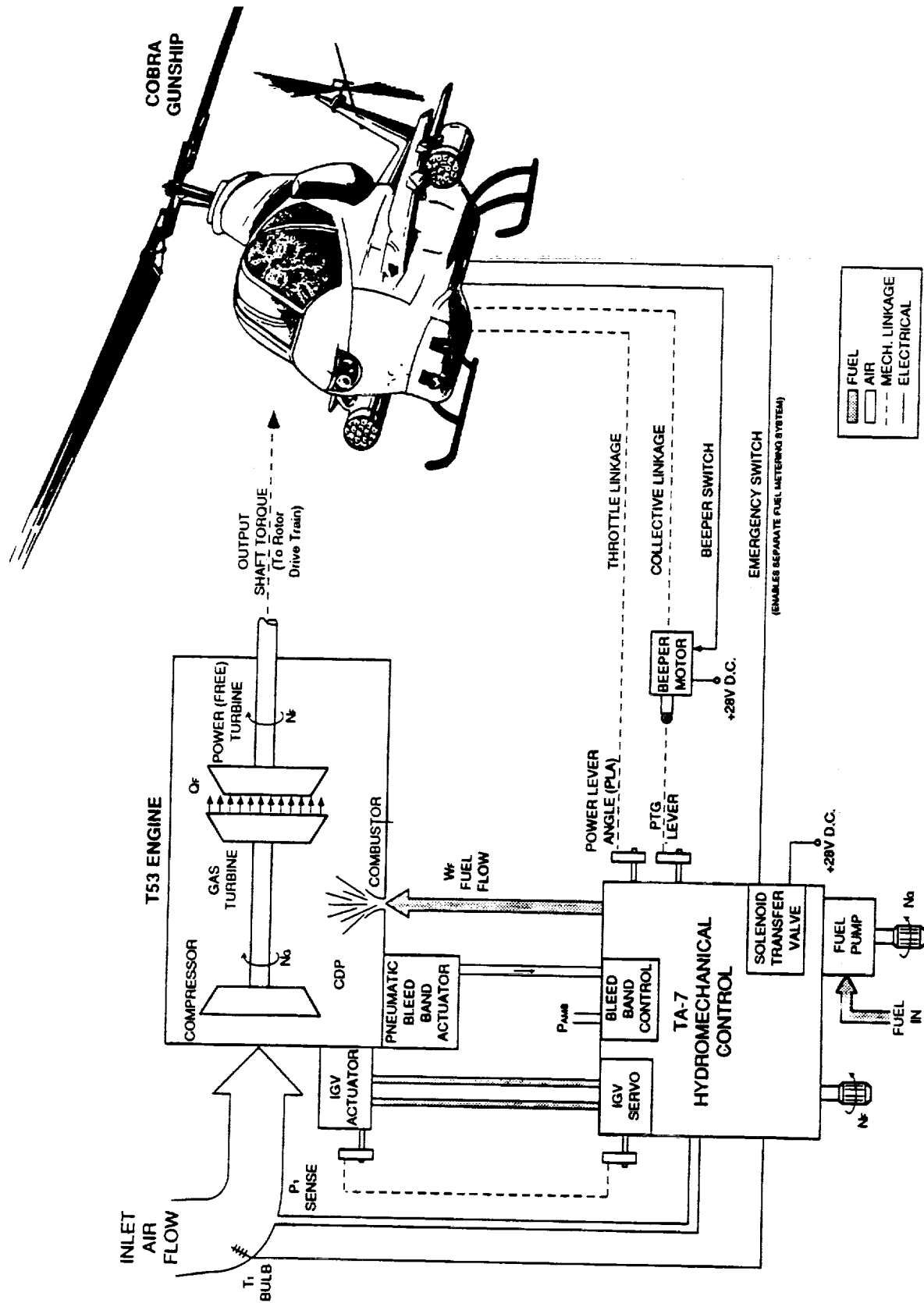
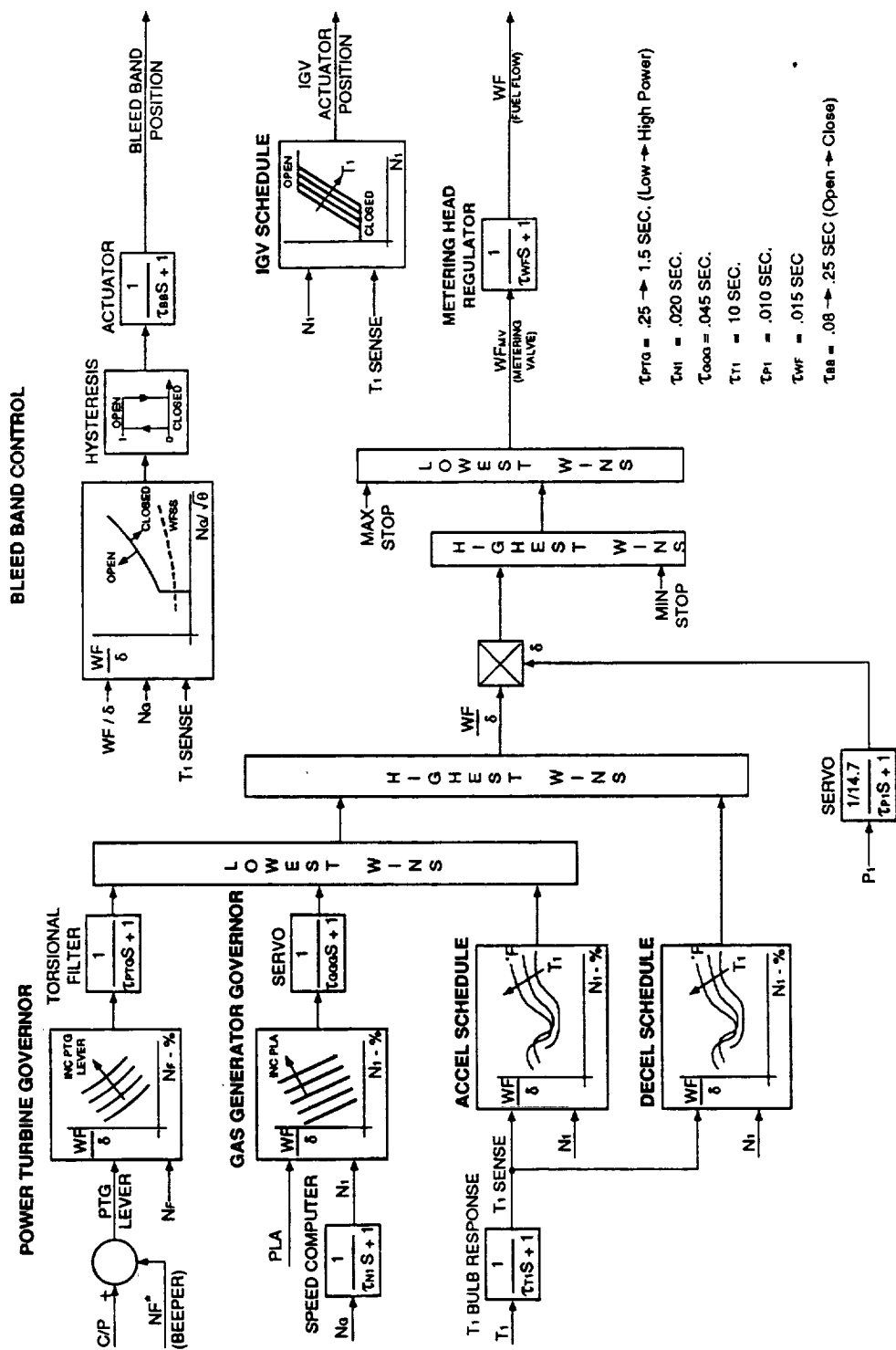


Figure 1

TA  
AUG 64 D



TA/153  
AC038A1 R

TA CONTROL SYSTEM . . . SIMPLIFIED FUNCTIONAL BLOCK DIAGRAM

Figure 2

The engine is further protected from blowout and overfueling by minimum and maximum metering valve stops. Fuel shutoff is accomplished via a separate PLA actuated valve not shown in the simplified functional block diagram of Figure 2.

The compressor inlet geometry actuator position is scheduled as a function of gas generator speed and T1. At low speed, the IGVs are closed to provide surge margin. At high speed, the IGVs are open to provide maximum engine efficiency. Actuator dynamics are fast and have been neglected for this study.

The two position (open or closed) compressor bleed band is controlled as a function of  $Wf/\delta$  and gas generator speed. Inlet temperature biases the N1 trip point to effectively result in a corrected  $N1/\theta$  schedule. For low  $Wf/\delta$  and low speeds, the bleed band remains open to preclude steady state engine surge. For high  $Wf/\delta$  and high speed, the bleed band is closed to provide maximum engine efficiency. During acceleration transients (i.e., high  $Wf/\delta$  and low speed) the bleed band is open to preclude transient surge.

The separate, emergency backup fuel metering system has not been modeled. This system was not in effect during the rocket fire problems encountered in the field, and therefore including it in this study was deemed to be out of scope. The emergency backup fuel metering system consists of a separate metering valve, separate metering head pressure regulator and a solenoid actuated transfer valve that allows the pilot to switch between the primary and backup systems. The backup fuel metering valve is mechanically linked directly to the PLA lever. A more detailed description of this system is contained in the Preliminary Design Section as it provides a convenient interface to a FADEC system that can potentially solve the rocket fire, transient torque spike problem.

In summary, all of the features of the primary engine control have been modeled. In addition, the essential dynamics of the primary hydromechanical computer and fuel handling section have also been modeled. These are incorporated as non-linear functions in the actual simulation code but are depicted as linearized time constants in Figure 2 to give the reader a quick reference as to the response of the various control loops.

## Engine

The Textron Lycoming T53-L-703 engine is a 1500 SHP turboshaft engine consisting of a gas generator section and a power (or free) turbine that is coupled to the helicopter rotor drive train. Figure 1 shows a schematic of the system and defines speed, pressure, and temperature stations throughout the engine.

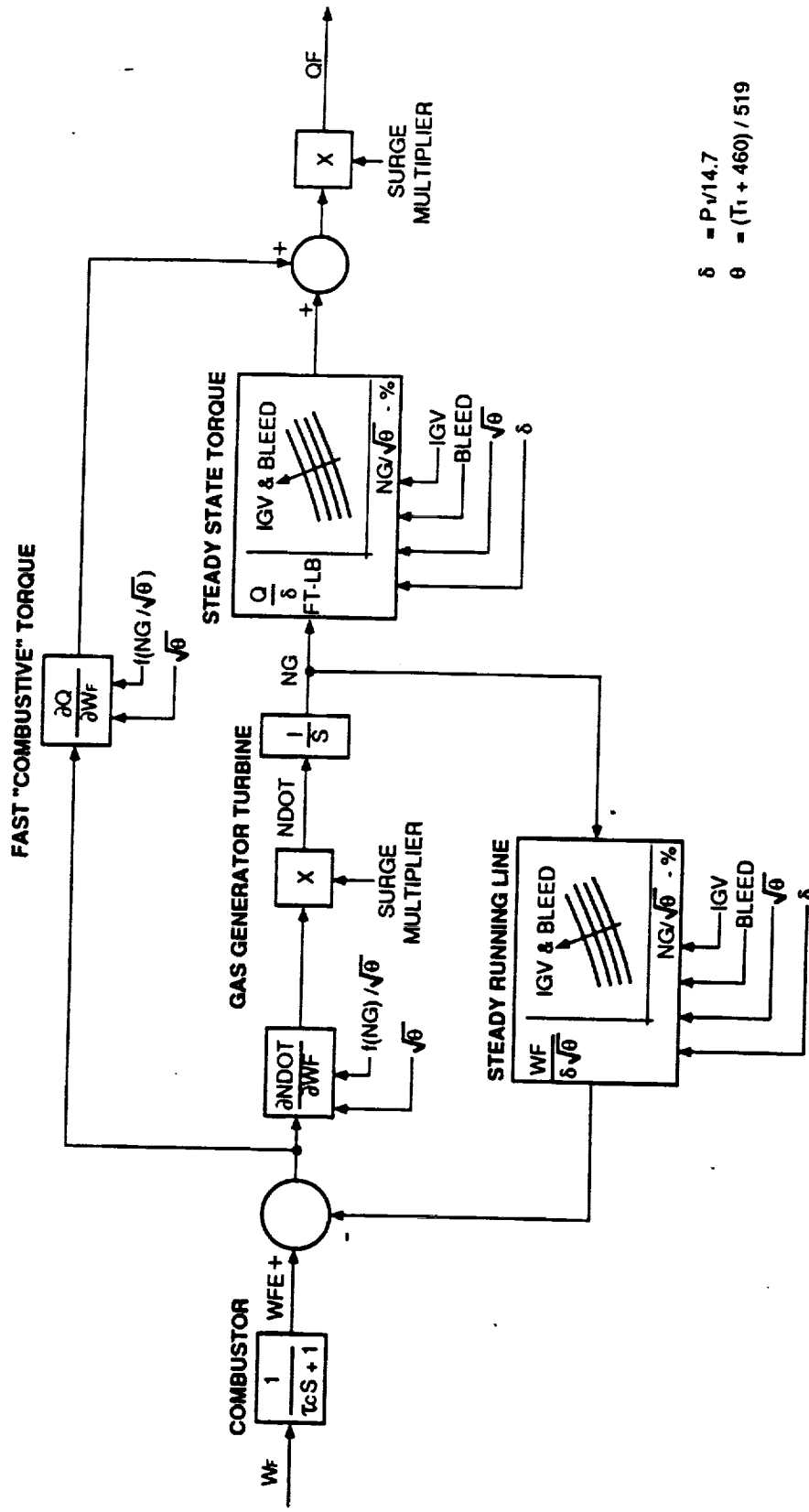
A functional block diagram of the T53 core (or gas generator) section of the engine is illustrated in Figure 3. This engine model is commonly referred by the industry as an excess torque model. Metered fuel flow is burned through relatively fast combustor dynamics and is compared to the engine steady state required to run fuel flow. Any difference generates excess torque and thus NDOT that accelerates or decelerates the gas turbine to a new operating condition.

The thermodynamic torque that is available to be applied to the free turbine,  $Q_F$ , is a sum of the core engine's steady state output torque and the fast transient torque that is available in the burned excess fuel flow that is not used by the gas turbine.

The engine model, as shown in Figure 3, is fully non-linear with engine performance a function of NG, BLEED, and IGV position.

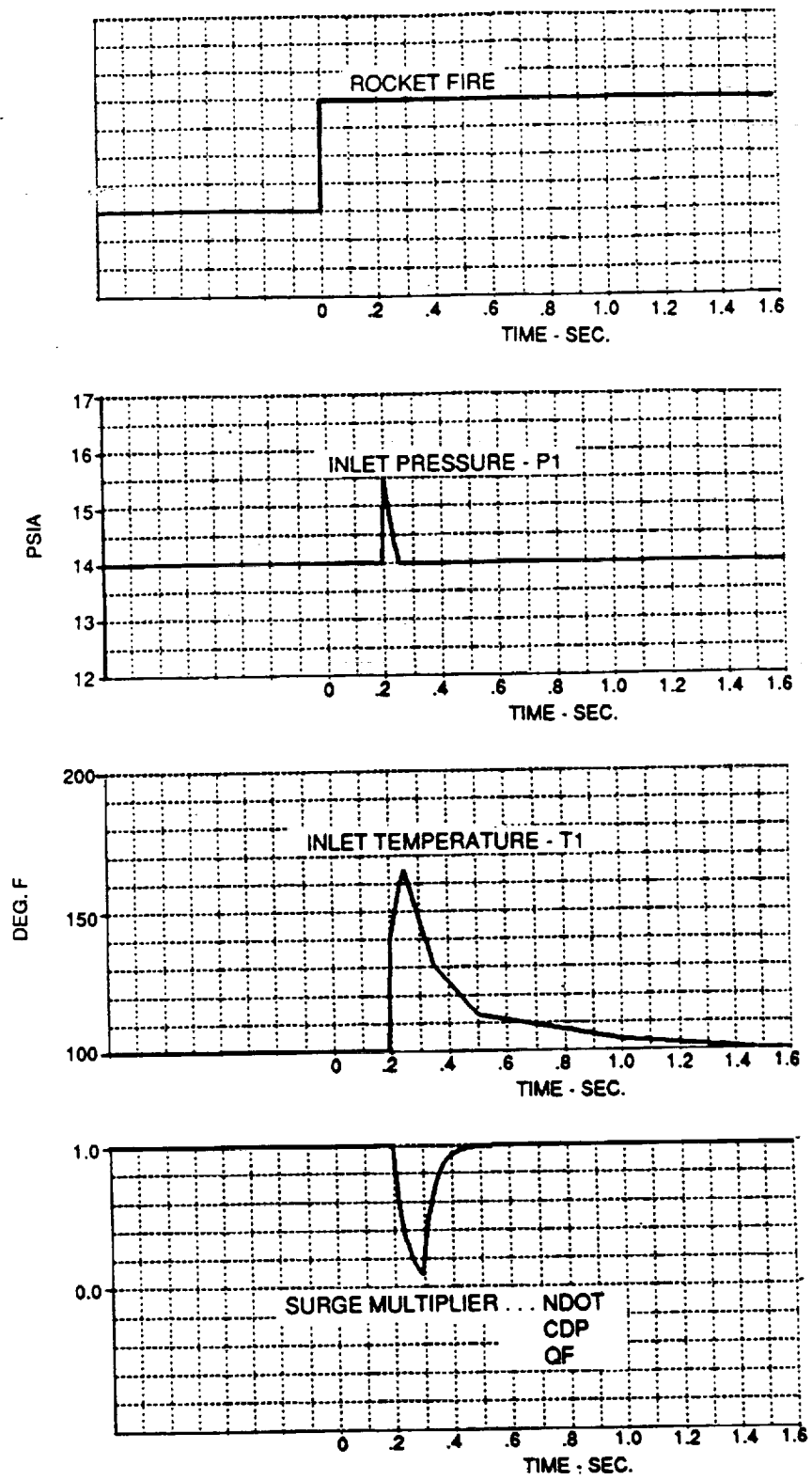
The model is corrected for inlet air pressure,  $P_1$ , and temperature,  $T_1$ . Therefore, the effects of rocket fire ingestion can be readily simulated by disturbing the model with  $P_1$  and  $T_1$  profiles as a function of time.

Surge is also modeled on an open loop basis by matching observed engine performance during an actual surge. The reduction in output torque,  $Q_F$  is simulated as shown in Figure 4. Incidence of hot gases at the inlet triggers the surge which then affects engine output for approximately 0.25 seconds.



**T53 CORE ENGINE . . . FUNCTIONAL BLOCK DIAGRAM**

Figure 3



ROCKET FIRE ENGINE SURGE SIMULATION  
Figure 4

## Rotor Drive Train

The rotor drive train consisting of the T53 power turbine, Cobra main rotor and tail rotor, and associated driveshaft and gearing is illustrated schematically in Figure 5. This diagram shows a 4 inertia/3 spring system that accurately models the main and tail rotor torsional modes. Since these modes are the prevalent frequencies observed on flight trace recordings of rocket fire surges, the simplified drive train model was deemed sufficient for the purposes of investigating fuel control effects.

A functional block diagram of the rotor drive train model is given in Figure 6. The model is non-linear in that the main rotor, tail rotor and free turbine damping terms are a function of flight condition. However, the block diagram is illustrated in a linearized fashion, to give the reader a quick reference as to the relative magnitude of damping terms present in the drive train.

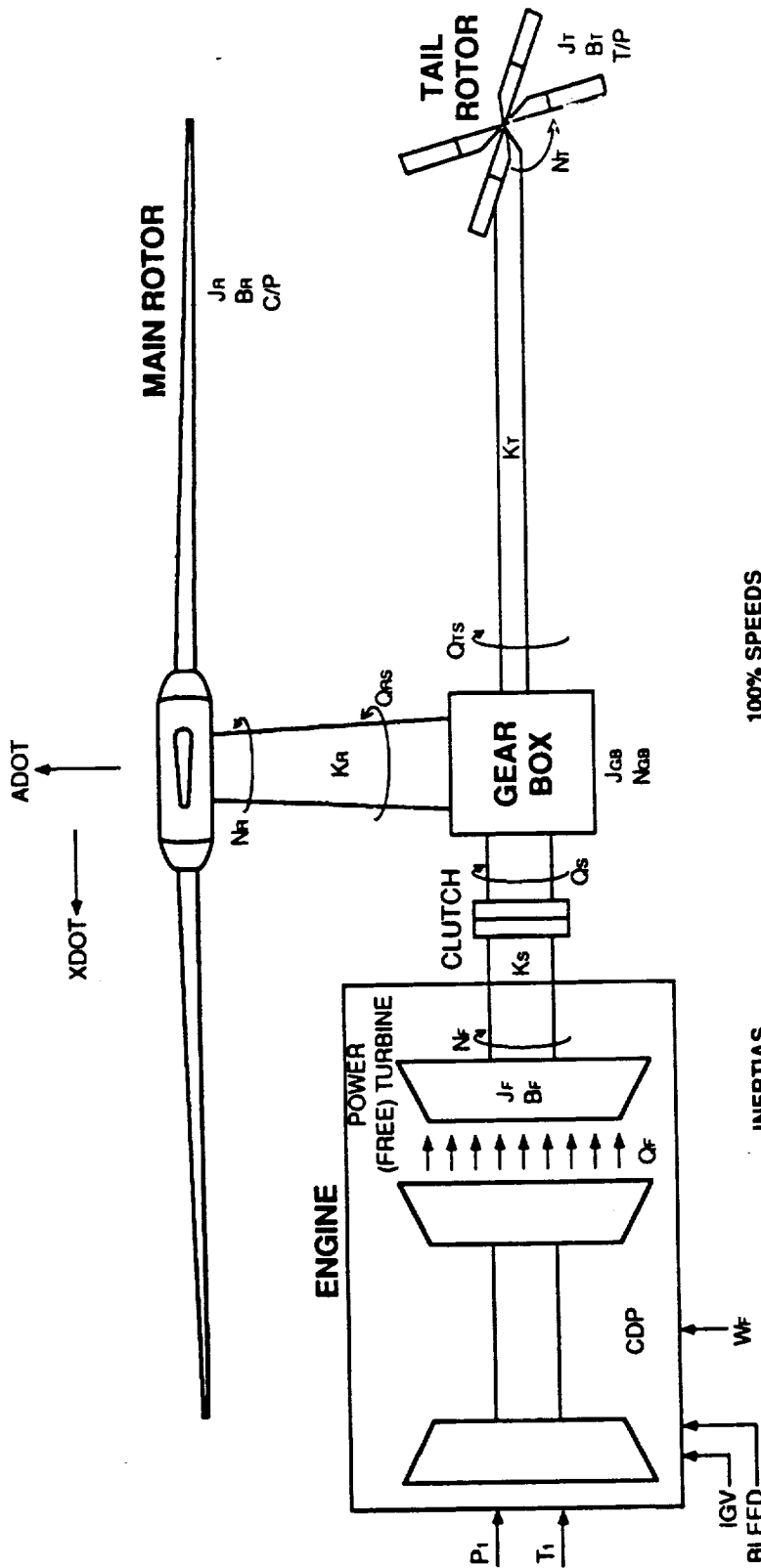
For the sea level hover, rocket fire condition, a linearized bode plot of the rotor drive train is given in Figure 7. This shows that the rotor system is very underdamped with a main rotor torsional mode of 2.9 Hz and 5.8% critical damping. The tail rotor torsional mode is 7.3 Hz and 2.5% of critical damping. Therefore, it should be no surprise that rapid disturbances to this system can excite the torsional modes and result in transient torque spikes.

## Airframe

A three degree of freedom airframe model including longitudinal, vertical and yaw degrees of freedom was utilized in the study. The airframe model also includes an automatic heading control that simulates the reaction of a human pilot. This model is proprietary to Chandler Evans, therefore, a more detailed description is not provided herein.

The airframe model was configured to the AH-1 helicopter and a few simulated flight maneuvers are enclosed to demonstrate that the model approximates AH-1 climb rate, descent rate, max airspeed, and heading control performance. These traces are enclosed in Figures 8 and 9. Based on these traces, the airframe model was deemed sufficient to evaluate the effect of rocket firings on the body states of the airvehicle.





**INERTIAS**  
 $J_F = 1.010$   
 $J_{GB} = .074$   
 $J_R = 5.900$   
 $J_T = .180$

SLUG · FT<sup>2</sup>

**SHAFTS**  
 $K_S = 10,000$   
 $K_R = 355.6$   
 $K_T = 316.8$

FT-LB / RAD

**DAMPING**  
 $B_F = .493$   
 $B_R = 2.26$   
 $B_T = .709$

FT-LB / RAD / SEC

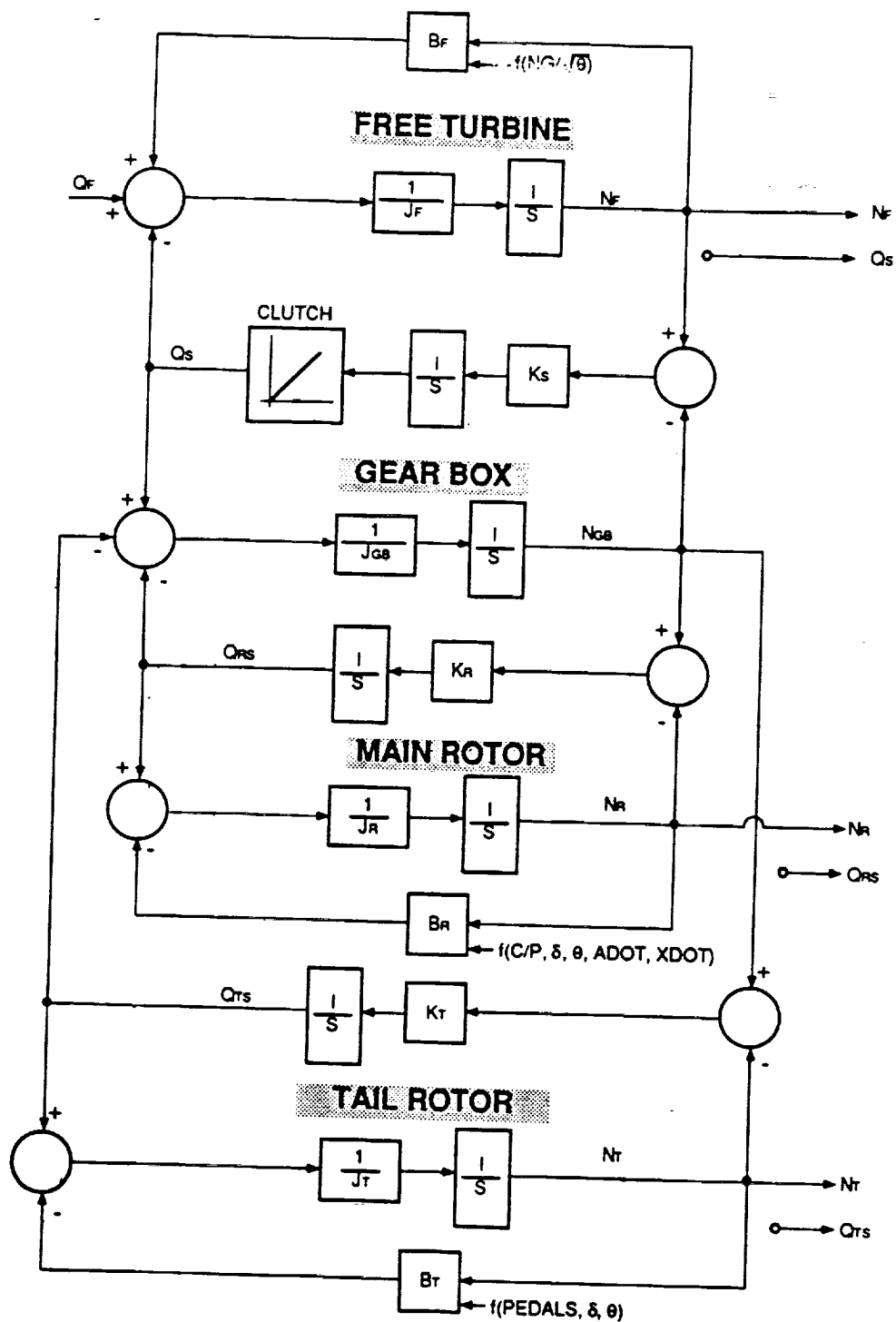
**100% SPEEDS**  
 $N_F = 6568$  RPM (SHAFT)  
 $N_T = 21,018$  RPM (TURBINE)  
 $N_R = 320$  RPM  
 $N_T = 1651$  RPM

**AIR SPEEDS**  
 $ADOT =$  CLIMB RATE  
 $XDOT =$  FORWARD SPEED

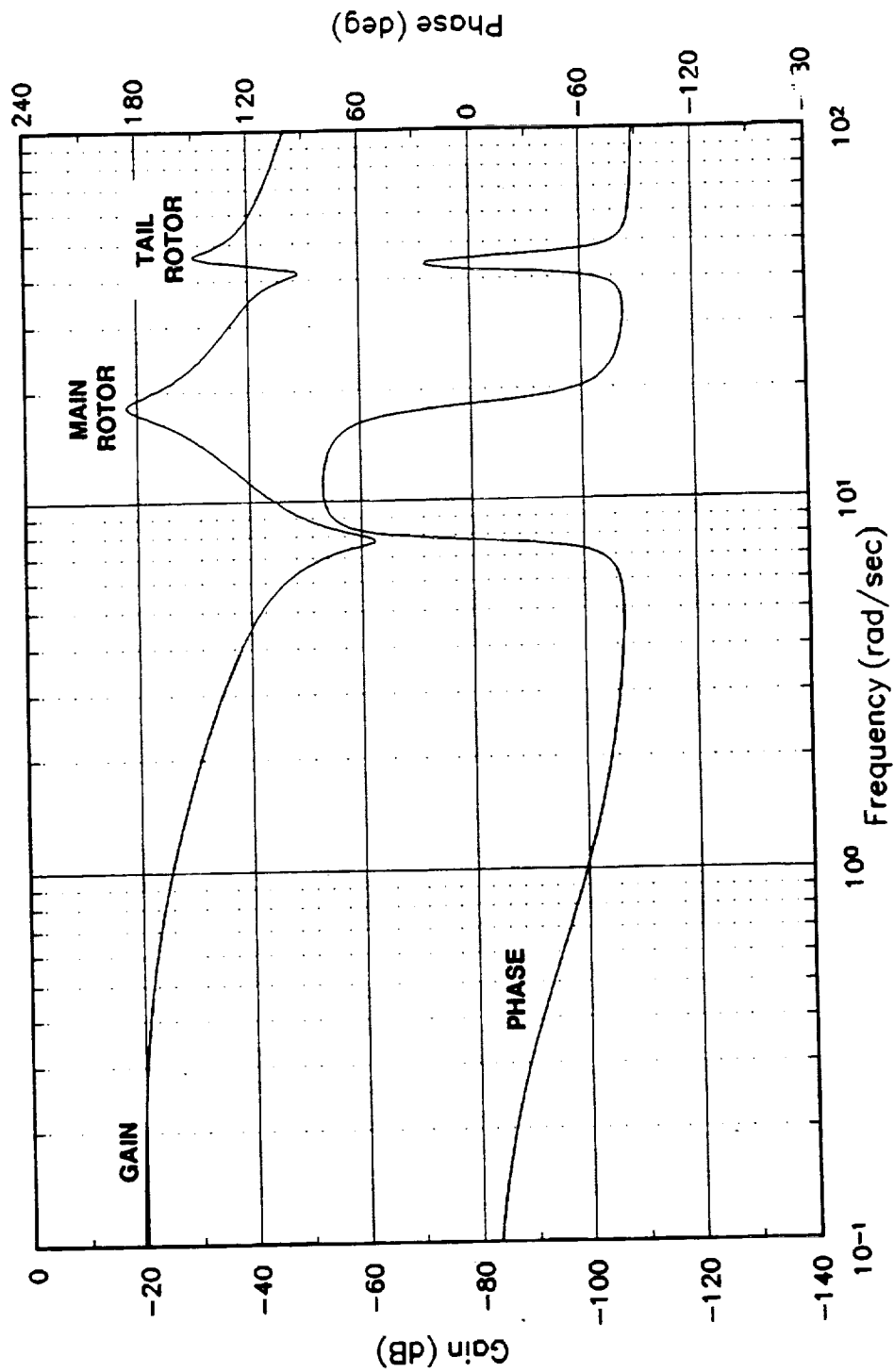
NOTE: ALL INERTIAS, SHAFTS, DAMPING  
 REFERRED TO POWER TURBINE  
 OUTPUT SHAFT SPEED. DAMPING  
 CALCULATED AT 98%  $N_G$

AH-1 / T53 ROTOR DRIVE TRAIN - SCHEMATIC

Figure 5

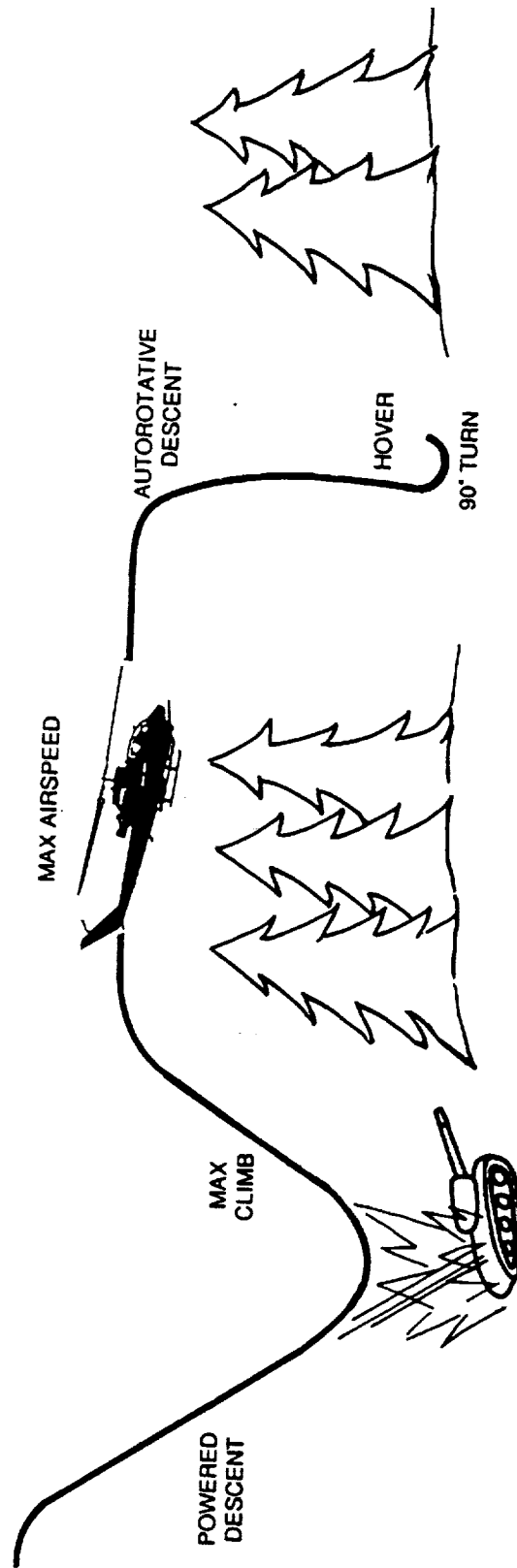


AH-1/T53 ROTOR DRIVE TRAIN - FUNCTIONAL BLOCK DIAGRAM  
Figure 6

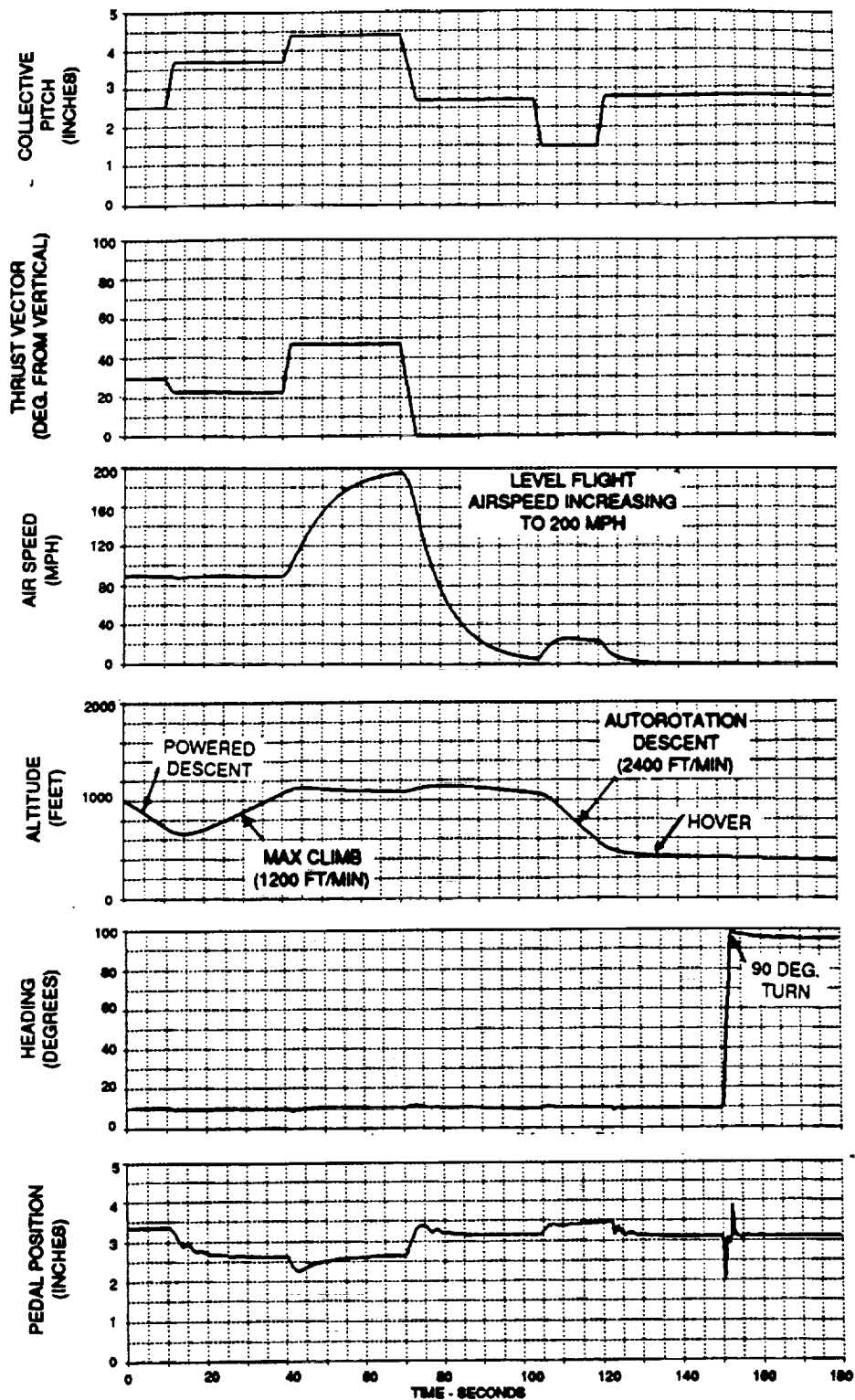


**AH-1/T53 ROTOR DRIVE TRAIN  
FREQUENCY RESPONSE - NF/QF**

Figure 7



**DEFINITION OF FLIGHT MANEUVER ... GUN RUN**  
 Figure 8



## SIMULATED FLIGHT MANEUVER . . . GUN RUN

Figure 9

## DISCUSSION OF RESULTS

The simulation model described in the previous section was used to evaluate the effects of rocket fire induced engine surges on the Cobra rotor drive train. The results are discussed in the following sections.

### Simulation of Rocket Fire Surges

Baseline flight test data was extracted from a U.S. Army Test and Evaluation Command (TECOM) final report TECOM Project No. 4-CO-230-000-016, "AH-1F Helicopter/Mark 66 2.75 inch Folding Fin Aerial Rocket Engineering Investigation", June 1991. Figure E-1 from this report is enclosed in Figure 10. This data shows a single engine surge as the result of a simultaneous firing of a pair of rockets (one from each pod). Engine inlet pressure and temperature, engine fuel flow and compressor discharge pressure, and rotor drive train torque spikes are all shown. Thus, a significant amount of data is present to correlate the simulation with test.

Figure 11 shows the simulation of the same event, and correlation with critical parameters is summarized in the table below.

Parameter	Test Data			Simulation		
	Hertz	Peak	Damping Ratio	Hertz	Peak	Damping Ratio
Main Rotor Torque	2.7	1400 ft-lb	3.2%	2.9	1700 ft-lb	4.7%
Tail Rotor Torque	7.0	340 ft-lb	3.4%	7.3	350 ft-lb	4.5%
Engine Shaft Torque	2.7	72 psi	3.5%	2.9	90 psi	4.4%
Fuel Flow Oscillation	2.7	± 35 pph	3.5%	2.9	± 40 pph	4.4%
Compressor Discharge Pressure Drop	N/A	90%	N/A	N/A	90%	N/A

$$\text{Note: } \zeta = \frac{100}{2\pi N} \ln \left( \frac{X_0}{X_N} \right)$$

where:

$\zeta$  = damping ratio, % of critical damping

$X_N$  = peak-peak amplitude of cycle  $N$

$X_0$  = peak-peak amplitude of first cycle

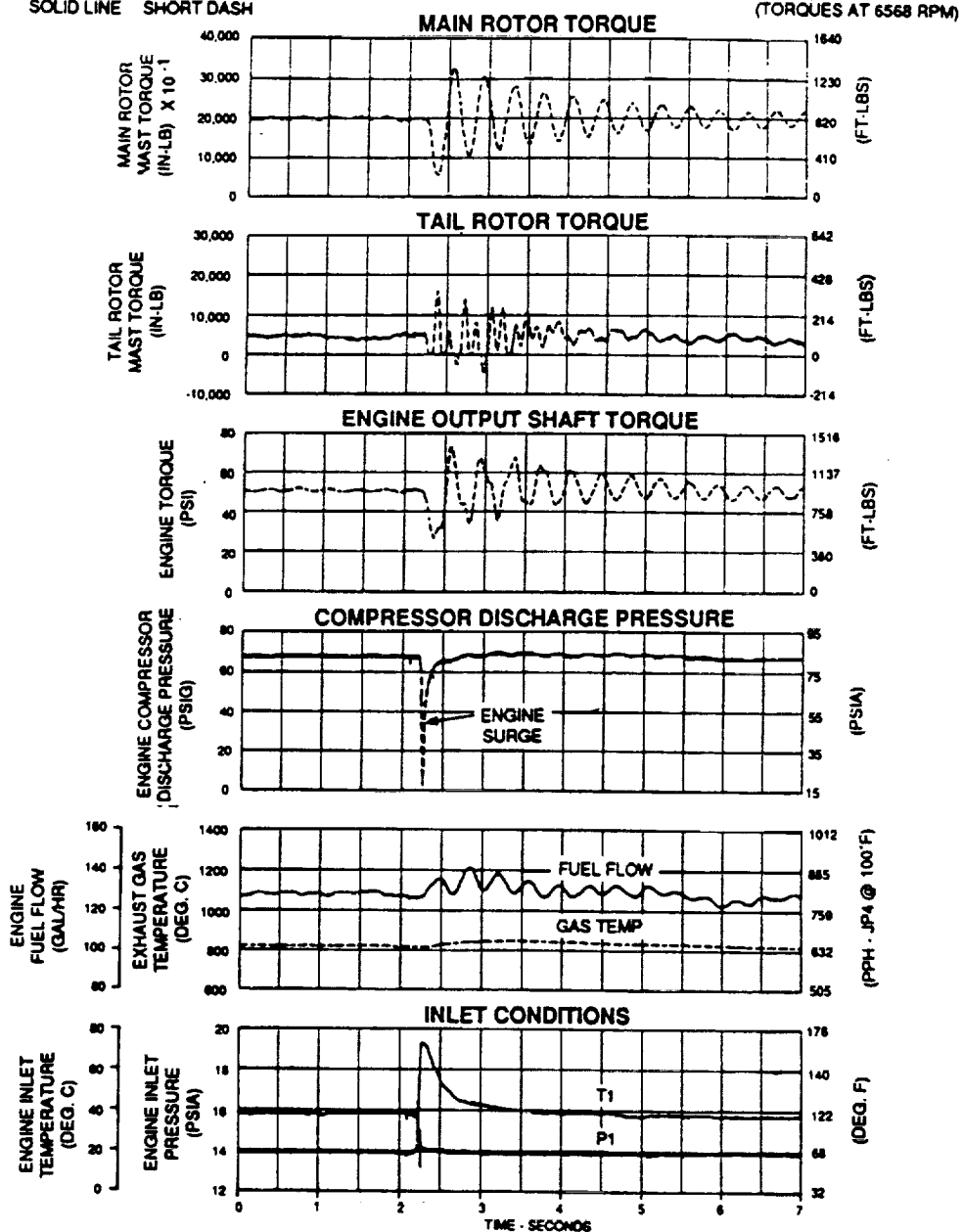
$N$  = number of cycles (10 typical)

Table I  
Correlation of Flight Test and Simulation of Rocket Fire Induced Engine Surge

AVG GROSS WEIGHT (LB)	CG LOCATION LONG (FS)	LAT (BL)	TRIM DENSITY ALTITUDE (FEET)	AVG OAT (DEG. C)	ROCKET FIRED	INLET SHIELD	FLIGHT CONDITION
9670	197.6 (MID)	0.1 RT	1300	26.0 80°F	2	NONE	5 KT LT SIDEWARD

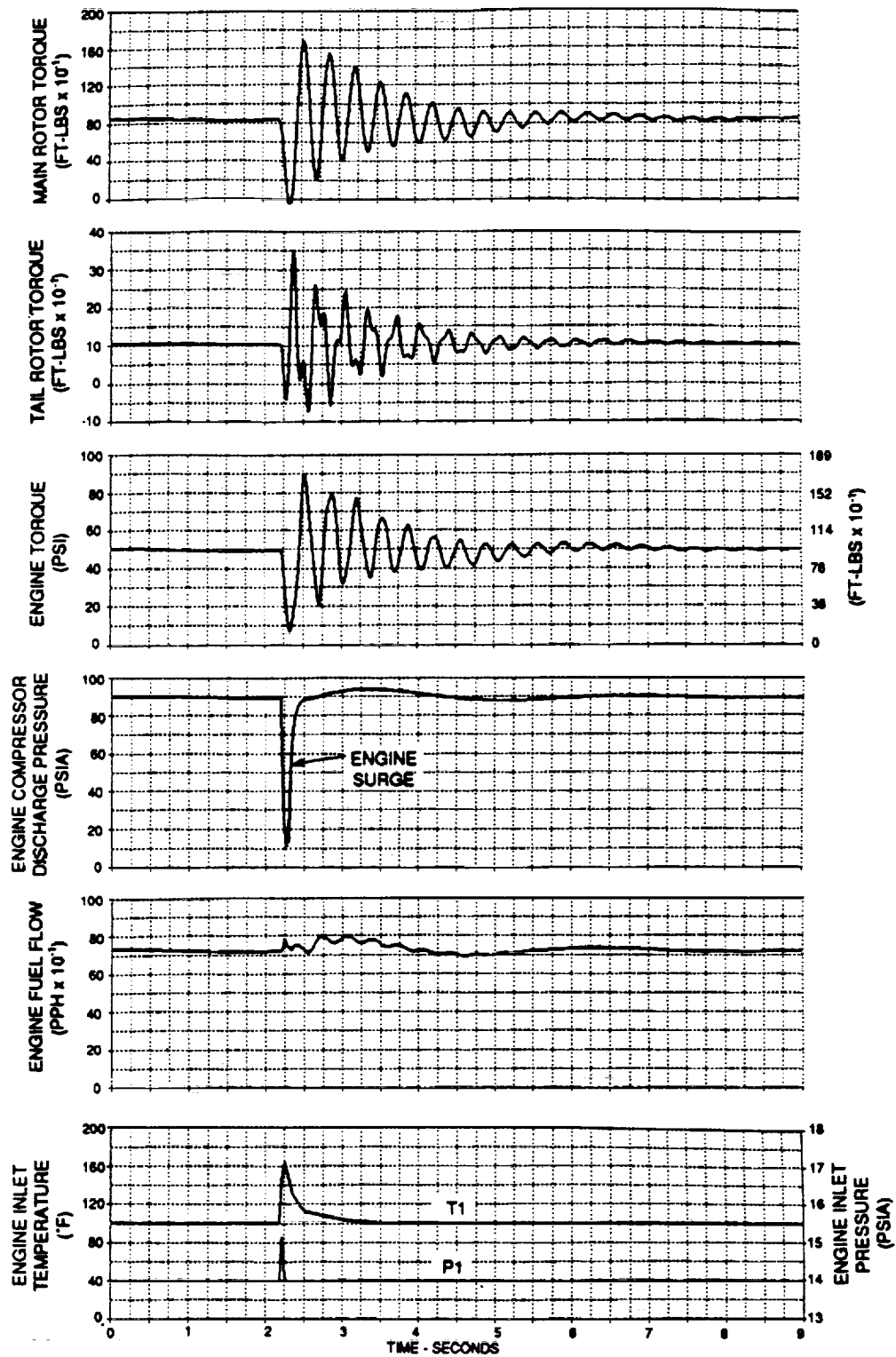
- NOTES: 1. MARK 66 ROCKET MOTORS USED.  
 2. M261 PODS INBOARD AND M65 LAUNCHERS OUTBOARD.  
 3. ENVIRONMENTAL CONTROL UNIT - OFF.  
 4. SKID HEIGHT - 10 FT.  
 5. AH-1F USA S/N 76-22600

SOLID LINE SHORT DASH



MK66 ROCKET FIRE FLIGHT TEST DATA (1 PAIR)

Figure 10



## SIMULATION OF MK66 ROCKET FIRE FLIGHT TEST (1 PAIR)

Figure 11



Peak tail rotor drive shaft torque, oscillation frequency, and damping ratio match almost exactly with the test data. These are the critical parameters, since a tail rotor drive shaft failure has occurred in the field as a result of rocket firings.

The main rotor torsional mode frequency and damping ratio match well considering the margin of error in reading the compressed time scale of the flight traces. However, the peak main rotor torque oscillation is 20% higher in the simulation. This also affects the simulated shaft torque which is the sum of main and tail rotor torques. Since the damping ratios of the actual vs. simulated drive train are close, the differences in the initial peak torque can be attributed to the simulated effect of engine surge on output torque.

The surge model illustrated in Figure 4 was left unchanged because the compressor discharge pressure drop as a result of surge and the resulting tail rotor spike due to the sudden disturbance to the rotor drive train were matched quite accurately. These are the most critical parameters for the study.

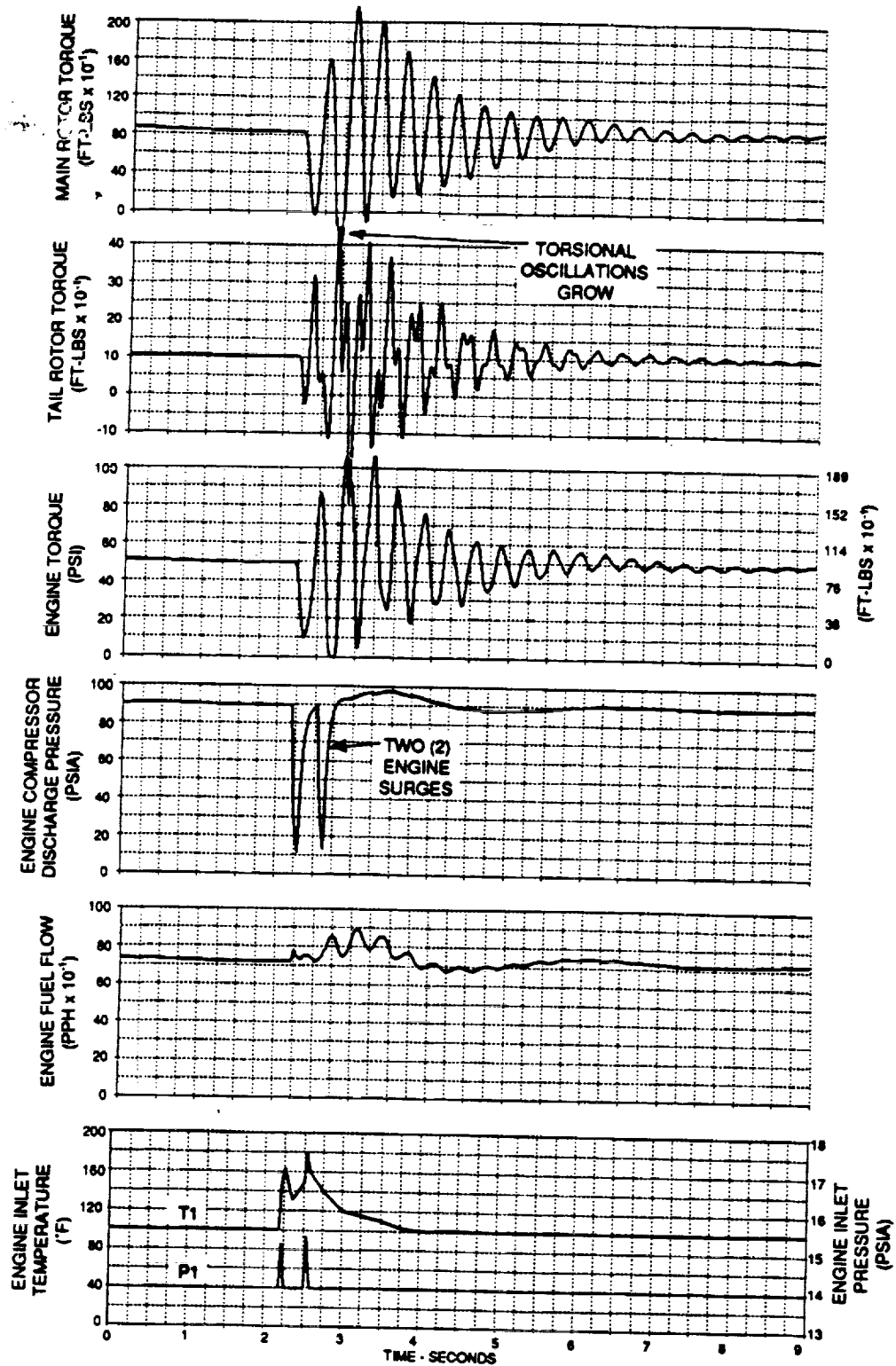
The single surge traces show that the rotor drive train is very lightly damped. The engine disturbance causes the drive train to ring with significant torque oscillations that require approximately 7 seconds to die out. This makes the rotor susceptible to a second or third surge disturbance that can occur due to multiple rocket firings. Furthermore, multiple rocket firings are performed at two pilot selectable frequencies that bracket the tail rotor resonant mode as shown in the table below.

Parameter	Frequency (Hz)
Main Rotor Torsional Mode	2.9
Slow Rocket Fire	6.3
Tail Rotor Anti-Resonance	6.7
Tail Rotor Torsional Mode	7.3
Fast Rocket Fire	8.3

**Table II**  
**Rocket Fire Frequency vs. Rotor Drive Train Torsional Modes**

Therefore, multiple rocket firings have a very good chance of amplifying torque spikes. Figure 12 illustrates a simulated, multiple rocket firing. Three rocket fires at the slow frequency result in two engine surges. As expected, the torsional oscillations are amplified beyond the normal tail rotor operating shaft torque limit.

The effect of the fuel control and modifications to the control system to attenuate these torque spikes are discussed in the following section.



**SIMULATION OF MULTIPLE ROCKET FIRES (3 PAIR)**

Figure 12

### Potential Solution Using the Existing TA Hydromechanical Control

The contribution of the bill-of-material TA control on rotor drive train torque spikes is demonstrated by comparing the simulated flight test data of Figure 11 and the results of Figure 13 where fuel flow is held constant throughout the rocket fire transient. The drive train responses are very similar with peak torque oscillations nearly identical.

The TA control attenuates torsional frequencies which are present in the power turbine speed signal by virtue of its 1 second hydraulic lag in the power turbine governor. The control also does not respond to the short duration P1 and T1 inlet disturbances and does not directly sense engine compressor discharge pressure and shaft torque which drop off suddenly during an engine surge. Therefore, it can be concluded that the TA control has a negligible effect on rotor drive train torque spikes caused by rocket fire engine surges.

The fuel control system must be modified to actively prevent engine surge or to react to engine surge in some fashion to attenuate rotor drive train torque spikes.

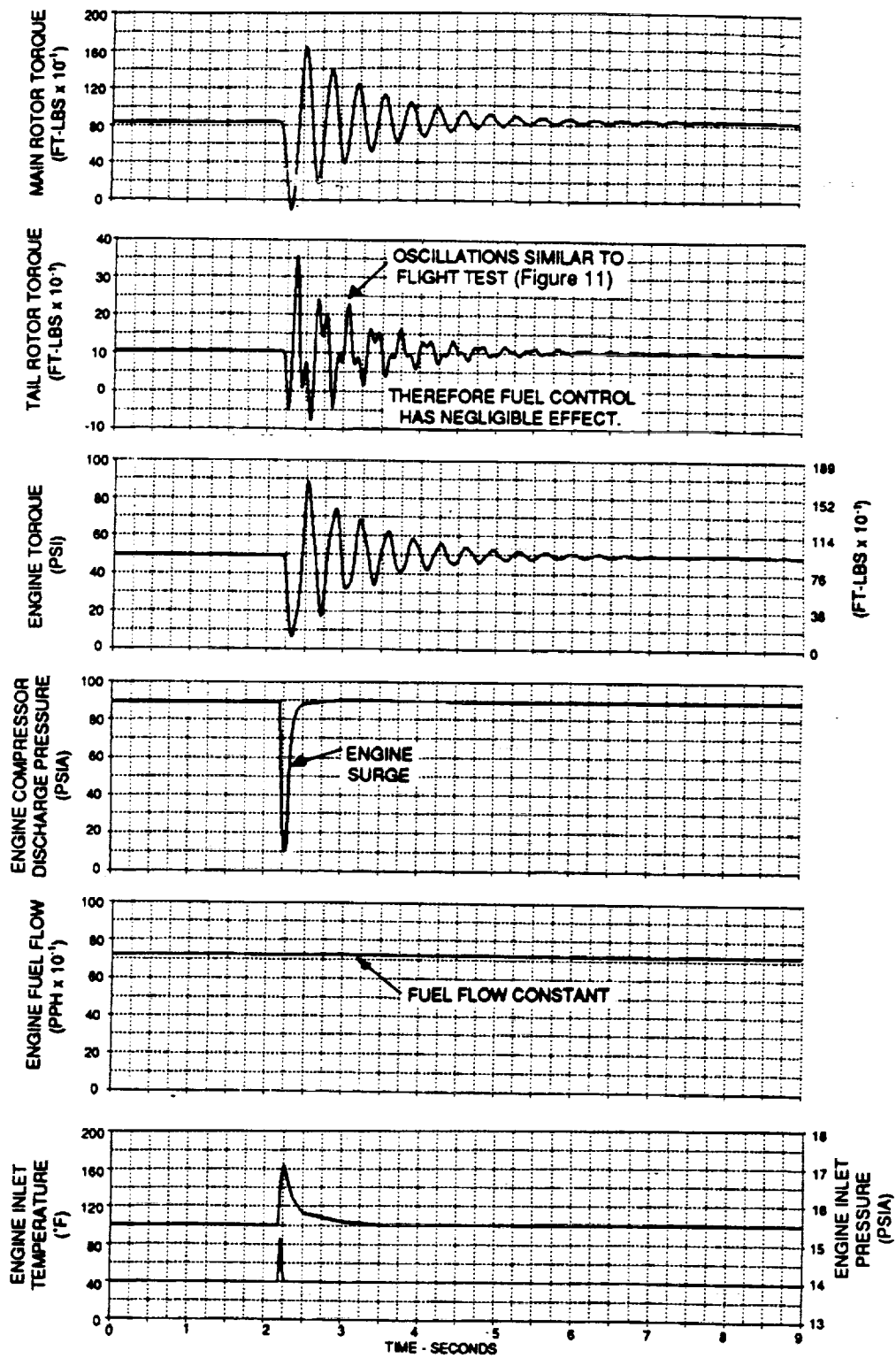
In an attempt to prevent surge, it was assumed that closure of the compressor inlet guide vanes (IGVs), when synchronized with rocket firings, could go a long way to block the amount of hot gases entering the engine and thereby preclude surge. The IGVs must be modulated between the open and closed position for each rocket fire because closing down the IGVs for a prolonged time period would degrade engine power and cause loss of rotor speed and helicopter lift.

Figure 14 illustrates the effect of modulating IGVs for a 19 shot, multiple rocket fire salvo. Engine surge is not triggered. However, the repeated IGV torque disturbances near the tail rotor frequency excite the lightly damped Cobra rotor drive train. Tail rotor torque spikes are amplified to an unacceptable level. Therefore, the rapid modulation of IGVs to preclude surge is not recommended as a viable solution.

Another possible alternative to alleviating the rocket fire torque spikes via the TA fuel control is to recover from engine surge in a smooth fashion. Engine output torque could be held down upon detection of surge, thereby reducing the tail rotor drive shaft torque spike.

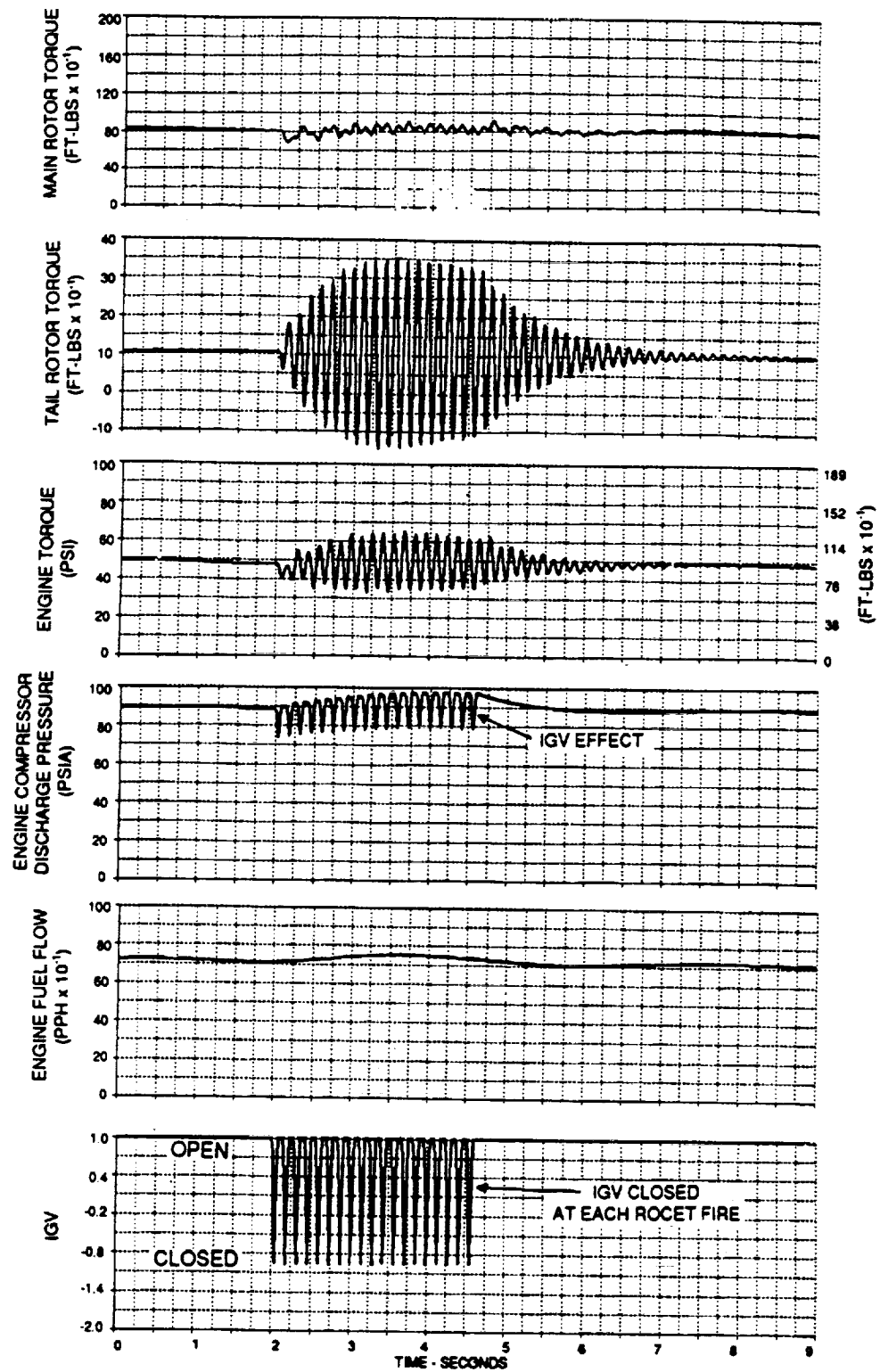
Figure 15 illustrates the simulation of a single rocket fire with IGV closed immediately upon detection of surge. The resulting tail rotor torque spike is similar (within 15%) to the simulated flight test data of Figure 11.

The IGV input is essentially too late, the rotor drive system resonates at too high a frequency (7.3 Hz). Shaft torque rebounds from the initial drop in torque due to engine surge before the IGVs can do much about it.



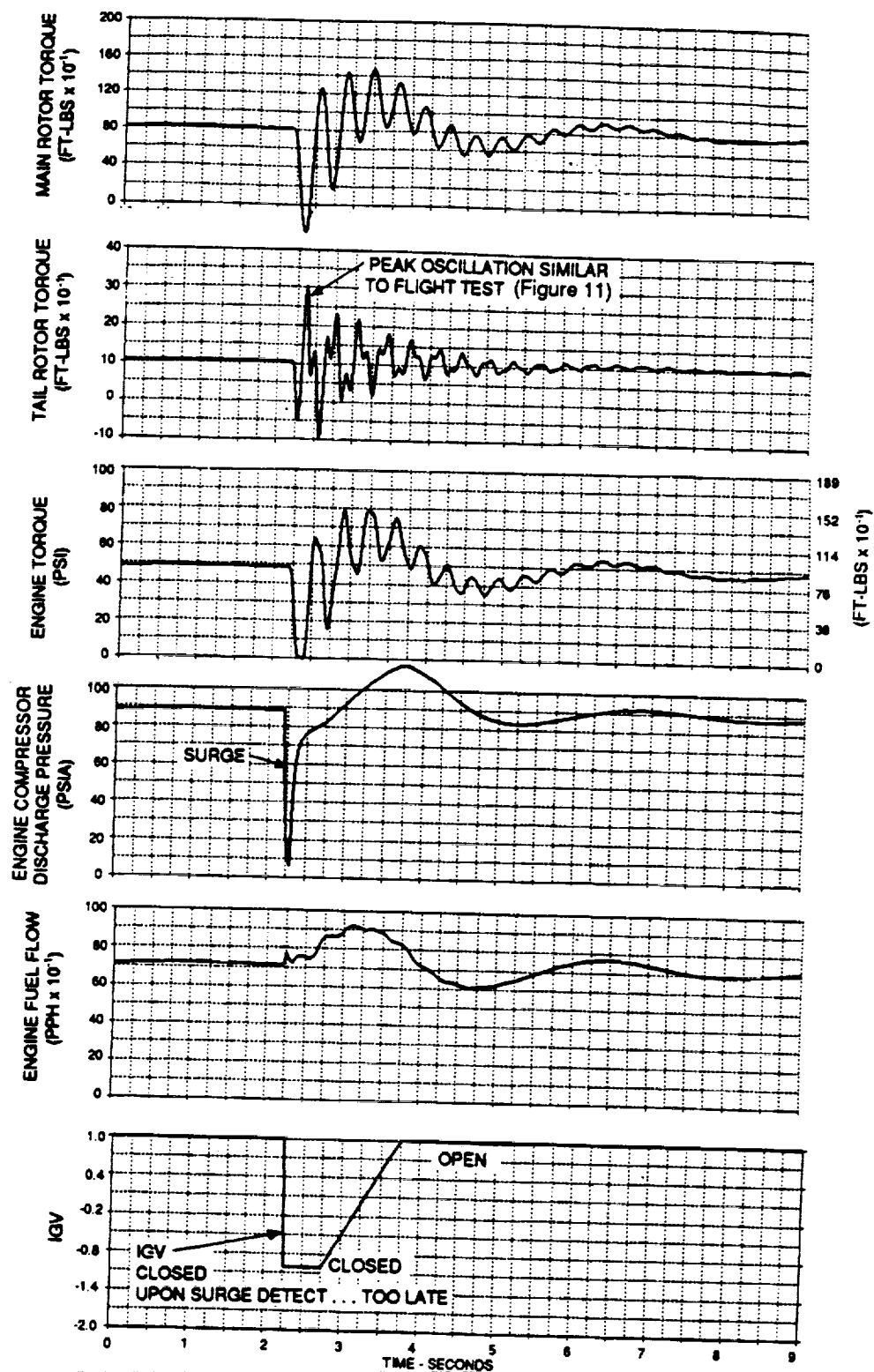
**SIMULATION OF ROCKET FIRE FLIGHT TEST (1 PAIR)**  
**(With Fuel Flow Constant)**

Figure 13



**SIMULATION OF MULTIPLE (19) ROCKET FIRES  
(With IGV Synched to Rocket Fire)**

Figure 14



**SIMULATION OF ROCKET FIRE FLIGHT TEST (1 PAIR)**  
 (With IGV Synched to Surge)

Figure 15

In the simulation results of Figure 15, zero time delay was assumed for surge detection and the IGV actuator was assumed to be instantaneous. In actual practice, a minimum of 0.1 second of reaction time must be added which corresponds to 3/4 of a tail rotor resonant cycle. This would degrade the results of Figure 15 even more. Therefore, it can be concluded that reacting to surge is too slow to preclude tail rotor drive shaft torque spikes.

In summary, the attempts to alleviate the drive train resonances in an "open loop" fashion by triggering off the rocket fire signal or by detecting surge are not viable solutions. The corrective action taken by the control must be very fast and even more importantly, it must be in direct opposition to the drive train resonances. If the corrective actions are not phased properly, they could do more harm than good by exciting the lightly damped torsional modes of the rotor drive train.

A "closed loop" method of attenuating drive train resonances is preferred. This requires a high bandwidth electronic control that eliminates the phase shift due to hydraulic servo lags that are present in the bill-of-material TA control.

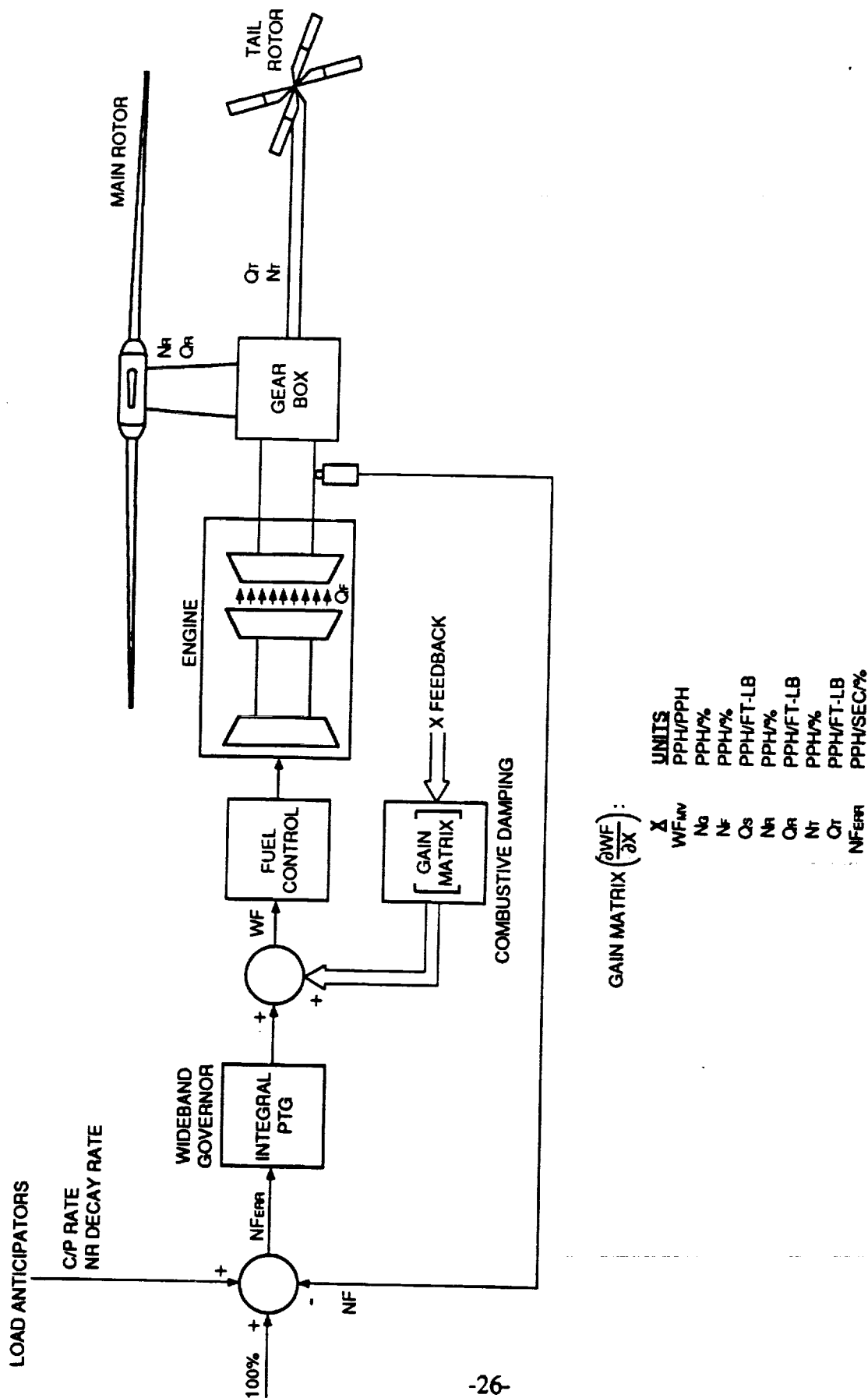
### **Active Damping via Electronic Control**

The architecture for a state feedback controller is illustrated in Figure 16. Additional states from the rotor drive train including main and tail rotor speeds and shaft torques are combined with typical engine control signals to create a fuel flow input that is in direct opposition to drive train resonances. The fuel flow input works through the fast combustive torque path of the engine as described in Figure 3 to modulate gas torque, QF, to provide damping at the 2.9 and 7.3 Hz torsional modes of the rotor drive train.

A frequency response plot of the AH-1/T53 rotor drive train, as defined in Figures 5 and 6, is included in Figure 17. As shown by the frequency response, the drive train is very lightly damped at the main and tail rotor torsional modes. With the electronic, combustive damping loop in effect however, the torsional modes are significantly attenuated. The performance of this controller during rocket fires is illustrated in Figures 18, 19, and 20.

For the single rocket fire in Figure 18 that emulates the flight test data, the peak tail rotor torque spike is significantly reduced. But more importantly, the drive train oscillations are damped out in one cycle. Therefore, multiple rockets can be fired off without fear of amplifying torsional oscillations.

Figure 19 shows the performance of the electronic controller during multiple rocket firings. The two rotor torque spikes caused by the two engine surges are contained within normal operating limits and the drive train oscillations are damped out in time for the next rocket fire. A bit more rotor speed droop (2%) than the baseline TA control is realized because the electronic control transiently lowers fuel flow to fight the drive train overtorque condition. The additional transient rotor speed droop should be of little consequence to the pilot since rotor speed recovers smoothly and quickly to the reference speed...as compared to the TA hydromechanical control which tends to overshoot and cause additional pilot workload.



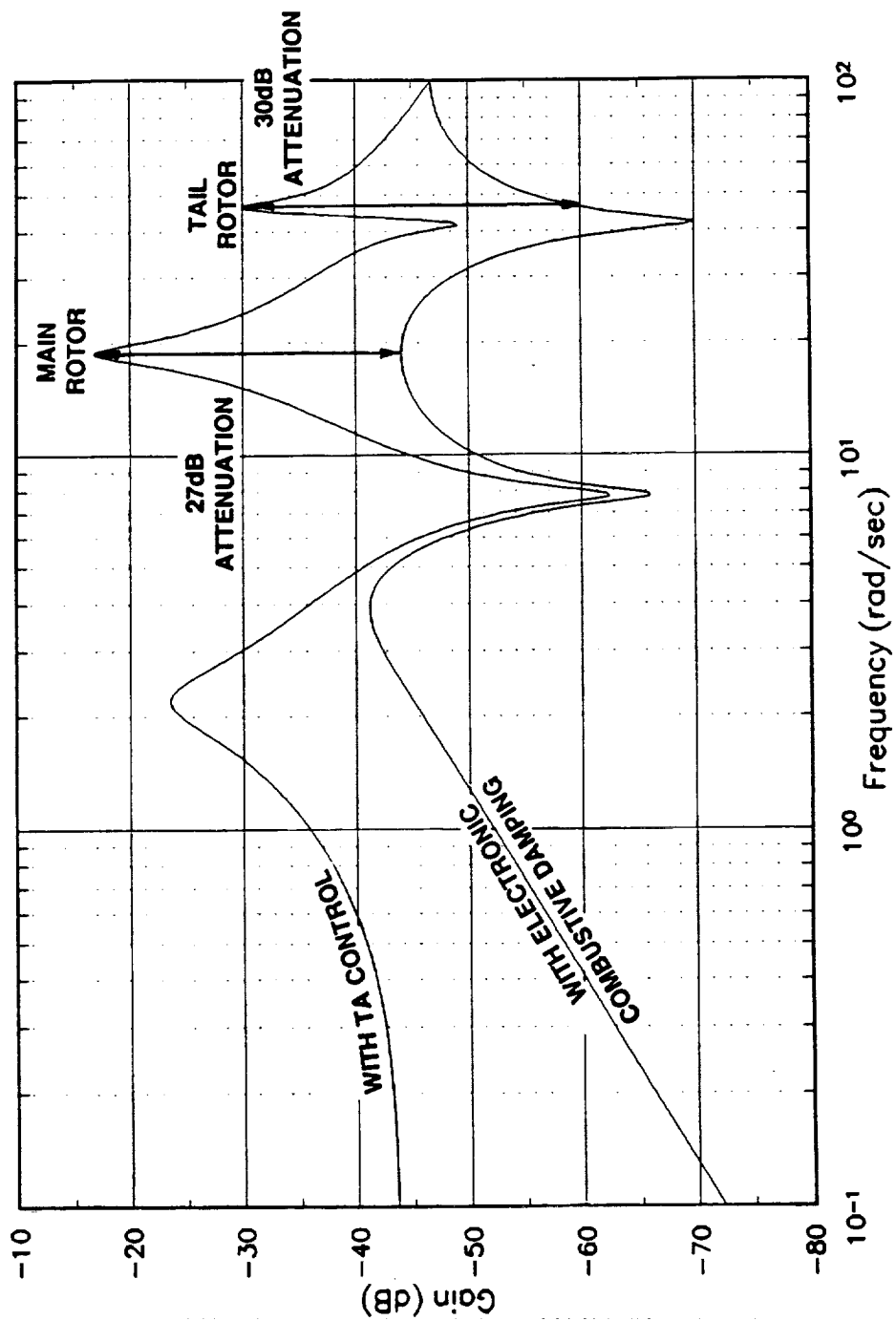
GAIN MATRIX  $\left( \frac{\partial WF}{\partial X} \right)$ :

$\Delta$	UNITS
WF <sub>inv</sub>	PPH/PPH
N <sub>g</sub>	PPH/%
N <sub>f</sub>	PPH/%
Q <sub>s</sub>	PPH/FT-LB
N <sub>r</sub>	PPH/%
Q <sub>r</sub>	PPH/FT-LB
N <sub>t</sub>	PPH/%
Q <sub>t</sub>	PPH/FT-LB
N <sub>FERR</sub>	PPH/SEC/%

COMBUSTIVE DAMPING BLOCK DIAGRAM

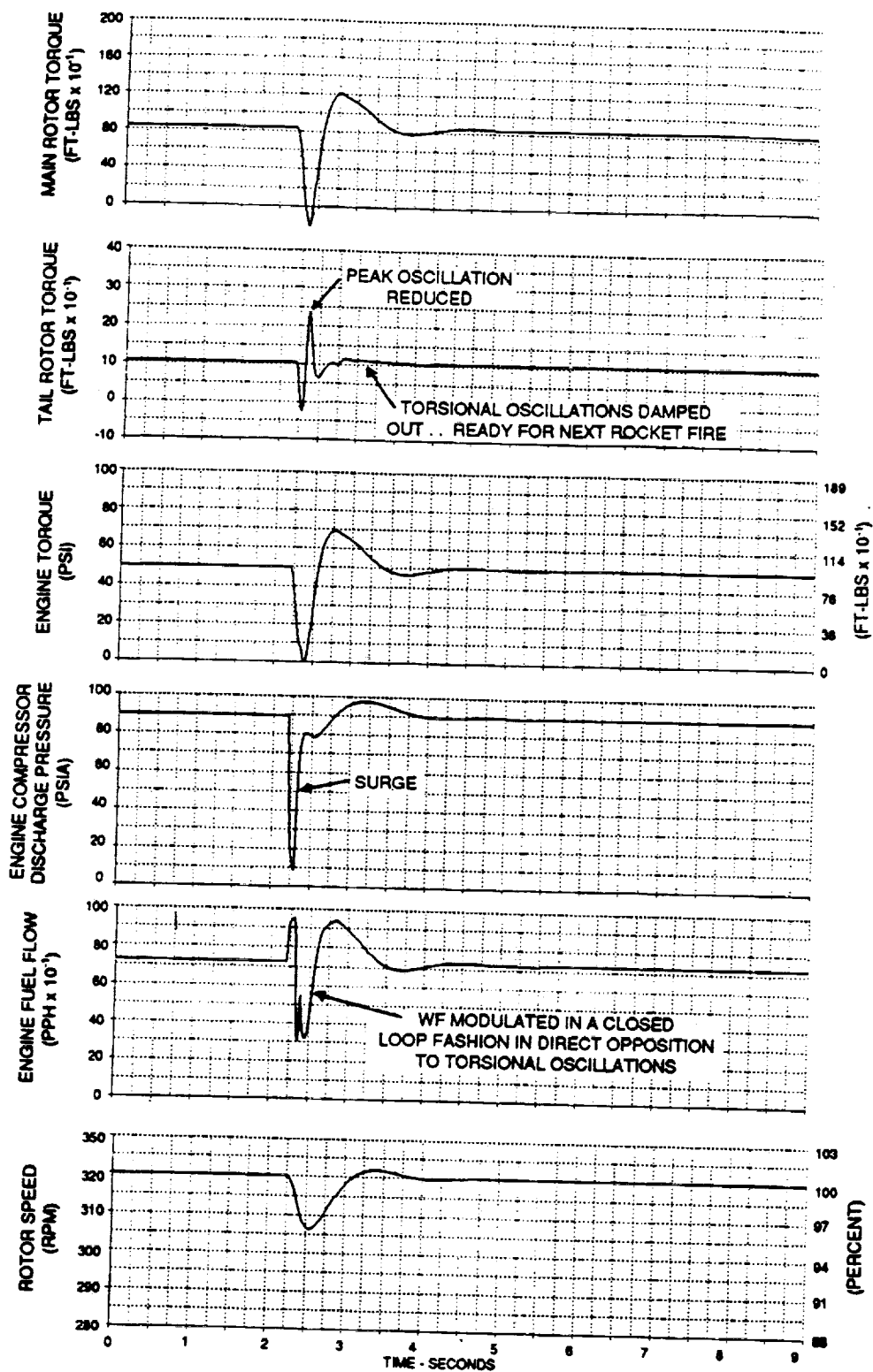
Figure 16





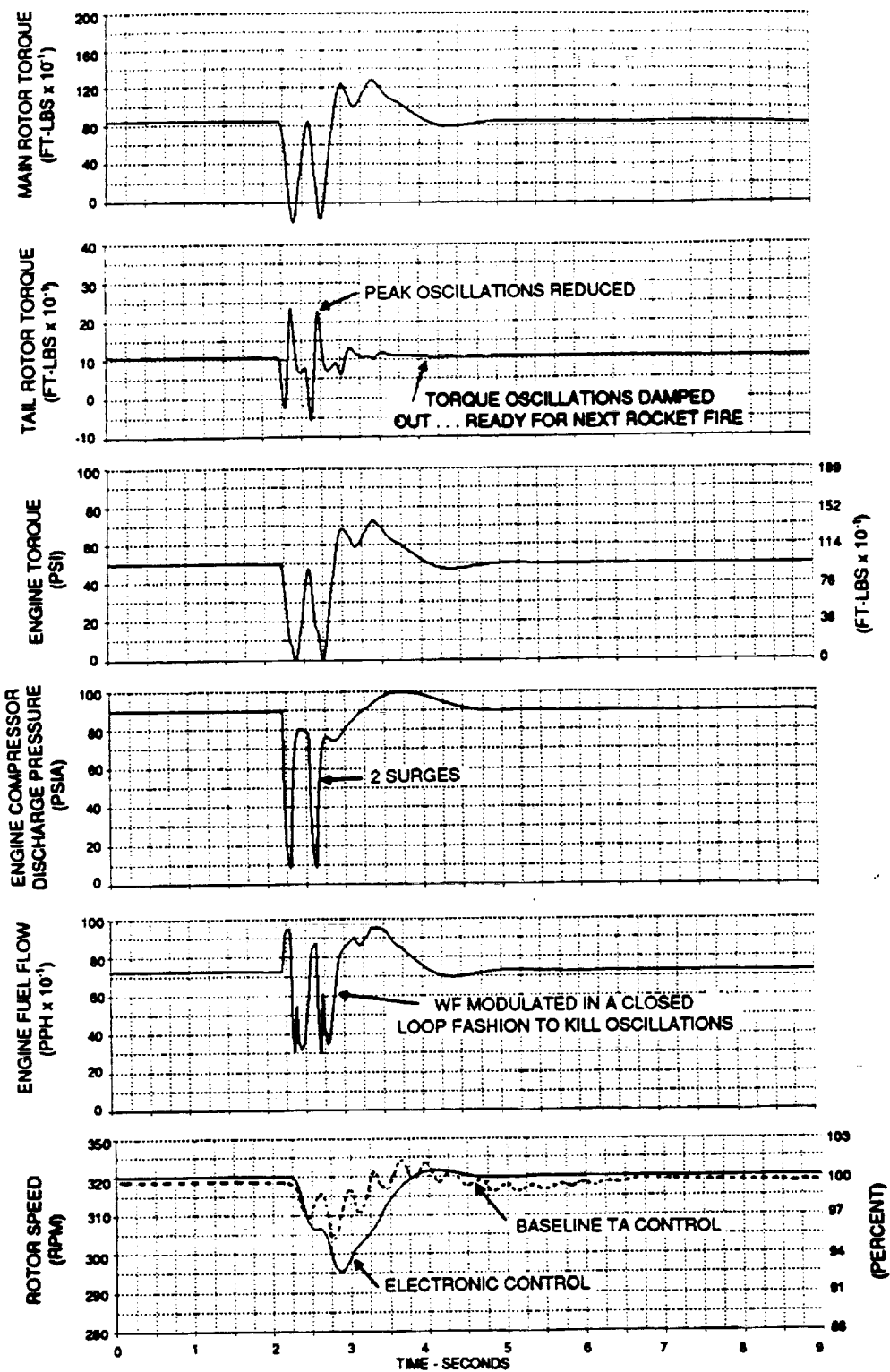
**EFFECT OF ACTIVE DAMPING ON AH-1/T53 ROTOR TORSIONALS  
TORQUE DISTURBANCE REJECTION - NF/QD**

Figure 17



**SIMULATION OF ROCKET FIRE FLIGHT TEST (1 PAIR)**  
**(With Electronic Combustive Damping)**

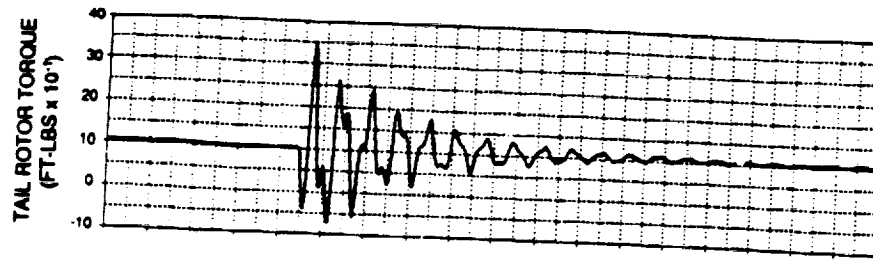
Figure 18



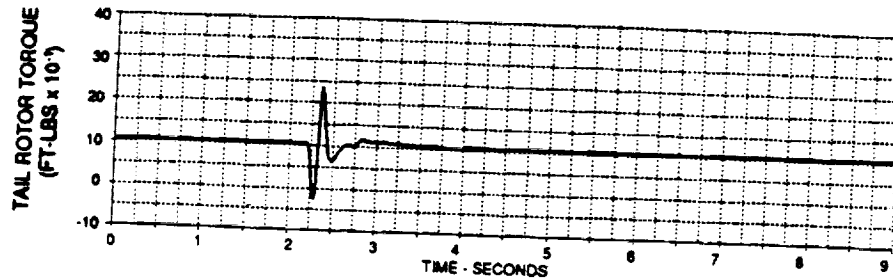
**SIMULATION OF MULTIPLE ROCKET FIRES (2 PAIR)**  
**(With Electronic Combustive Damping)**

Figure 19

### SINGLE ROCKET FIRE (1 PAIR)

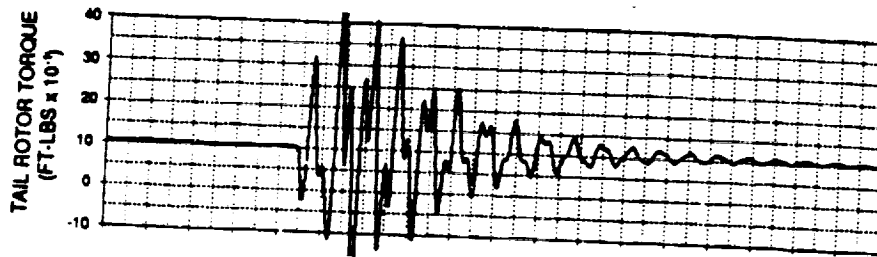


**BASELINE**

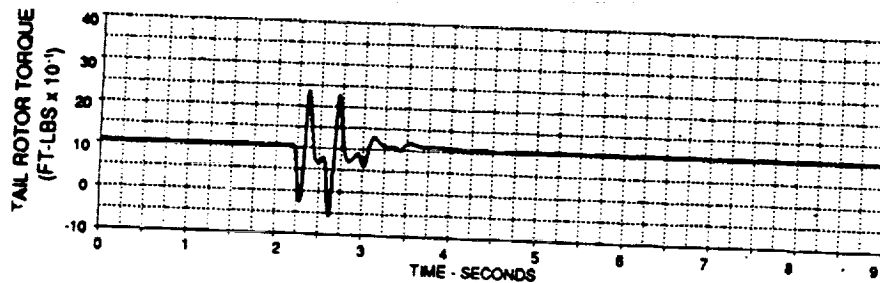


**COMBUSTIVE  
DAMPING**

### MULTIPLE ROCKET FIRES (2 PAIR)



**BASELINE**



**COMBUSTIVE  
DAMPING**

### EFFECT OF COMBUSTIVE DAMPING ON AH-1 ROTOR DRIVE TRAIN TORSIONALS

Figure 20

A summary of electronic combustive damping performance is given in Figure 20. Peak tail rotor torque spikes are attenuated by 25-40% for single and multiple rocket firings as compared to the baseline system. And, most importantly, tail rotor resonances are damped out quickly such that repeated rocket firings do not have a chance to amplify the drive shaft natural resonances and potentially damage the drive system.

### **Performance Benefits**

In addition to damping out the rotor drive train resonances, the electronic control provides a fast rotor speed control for normal operation. Figure 21 compares the frequency responses of the electronic Wideband Power Turbine Governor (PTG) with the bill-of-material TA hydromechanical control.

The NF/QD frequency response illustrates the improved disturbance rejection capability of the Wideband PTG. The effect of a ramp disturbance to the rotor drive train (i.e., collective pull/drop) causes rotor speed under Wideband PTG control to change by nearly 1/10 the amount of the TA control. The NF/NF frequency response shows the improved response of the speed control loop. The Wideband governor corrects speed errors 50% faster than the TA control.

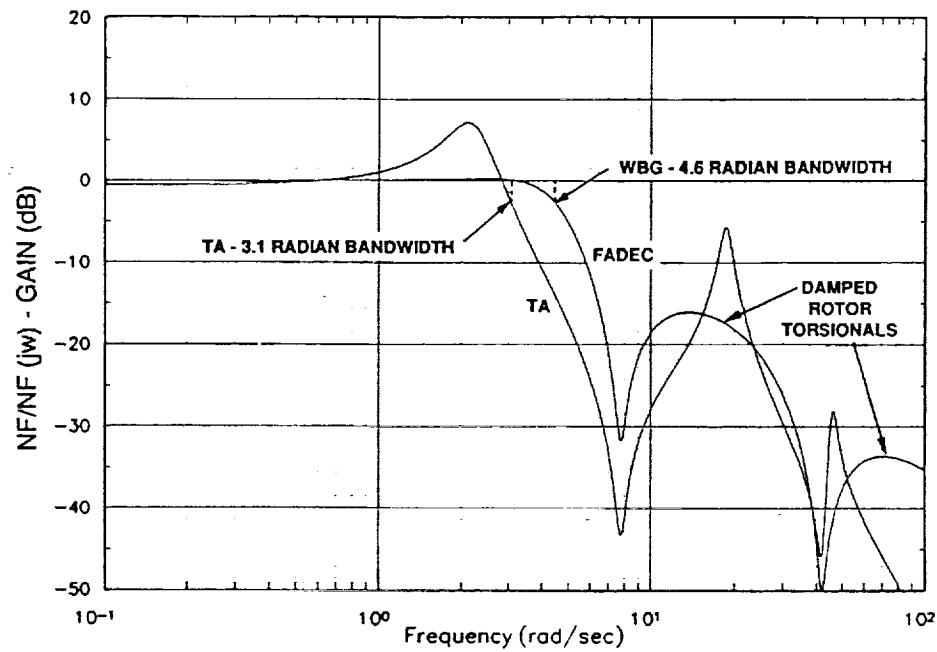
The effect of improved disturbance rejection and faster speed control results in a more agile and easier to fly helicopter as demonstrated by Figures 22 and 23.

Figure 22 illustrates a 2 second collective pull from a low power descent into a high power climb with the TA control on board. A 7.5% transient rotor speed droop is caused by a slow transition from Power Turbine Governor to the engine's accel fuel flow limit. This is primarily due to the 0.2 to 1.0 second hydraulic lag in the PTG servo that is designed to filter out torsional resonances and thereby maintain closed loop stability. This lag also causes the speed control loop to hunt a bit as it settles into a new operating condition. This is evident by the 20% torque overshoot and subsequent settling oscillations at high power.

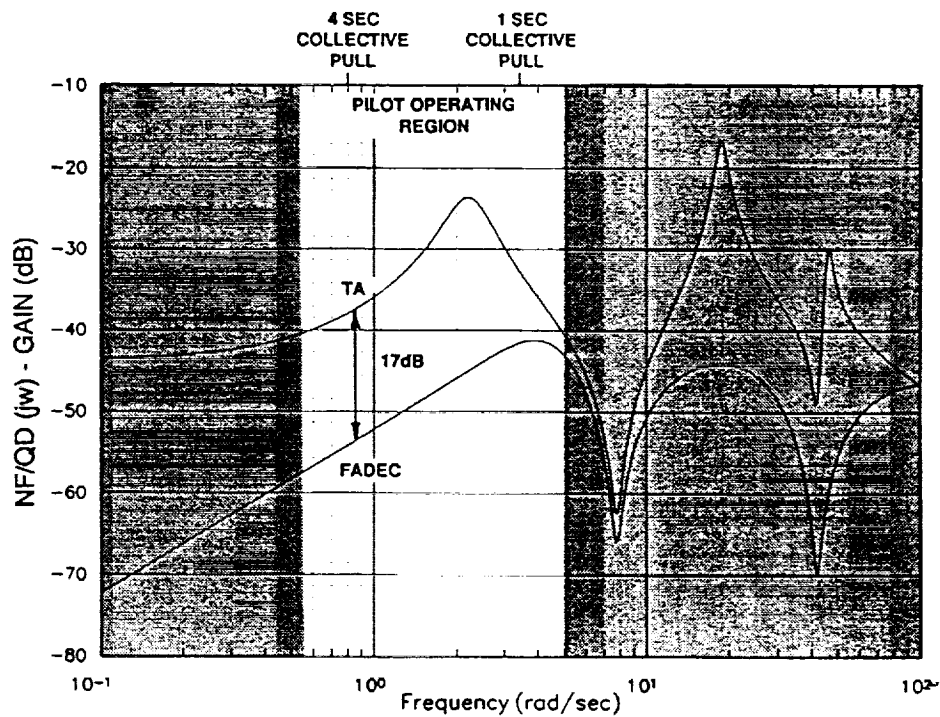
The net result of this speed and torque control performance is degraded helicopter maneuverability and increased pilot workload. Six (6) seconds are required to arrest the descent. And, the nose of the helicopter swings back and forth as the pilot is working the pedals to maintain heading. With this type of performance, it should be no surprise that the Cobra gets out-maneuvered in air-air combat against FADEC equipped airvehicles.

Figure 23 illustrates the same maneuver with the electronic Wideband PTG on-board. A fast transition from power turbine governing to the engine's accel limit is achieved which results in minimal rotor speed droop (1%). Torque overshoot is also minimal (4%) with no settling oscillation. Therefore, the descent is arrested in 3.5 seconds, and heading is maintained with little pilot workload.

These traces demonstrate that a significant improvement in aircraft maneuverability and handling qualities can be achieved by adding a FADEC system to the Cobra helicopter.

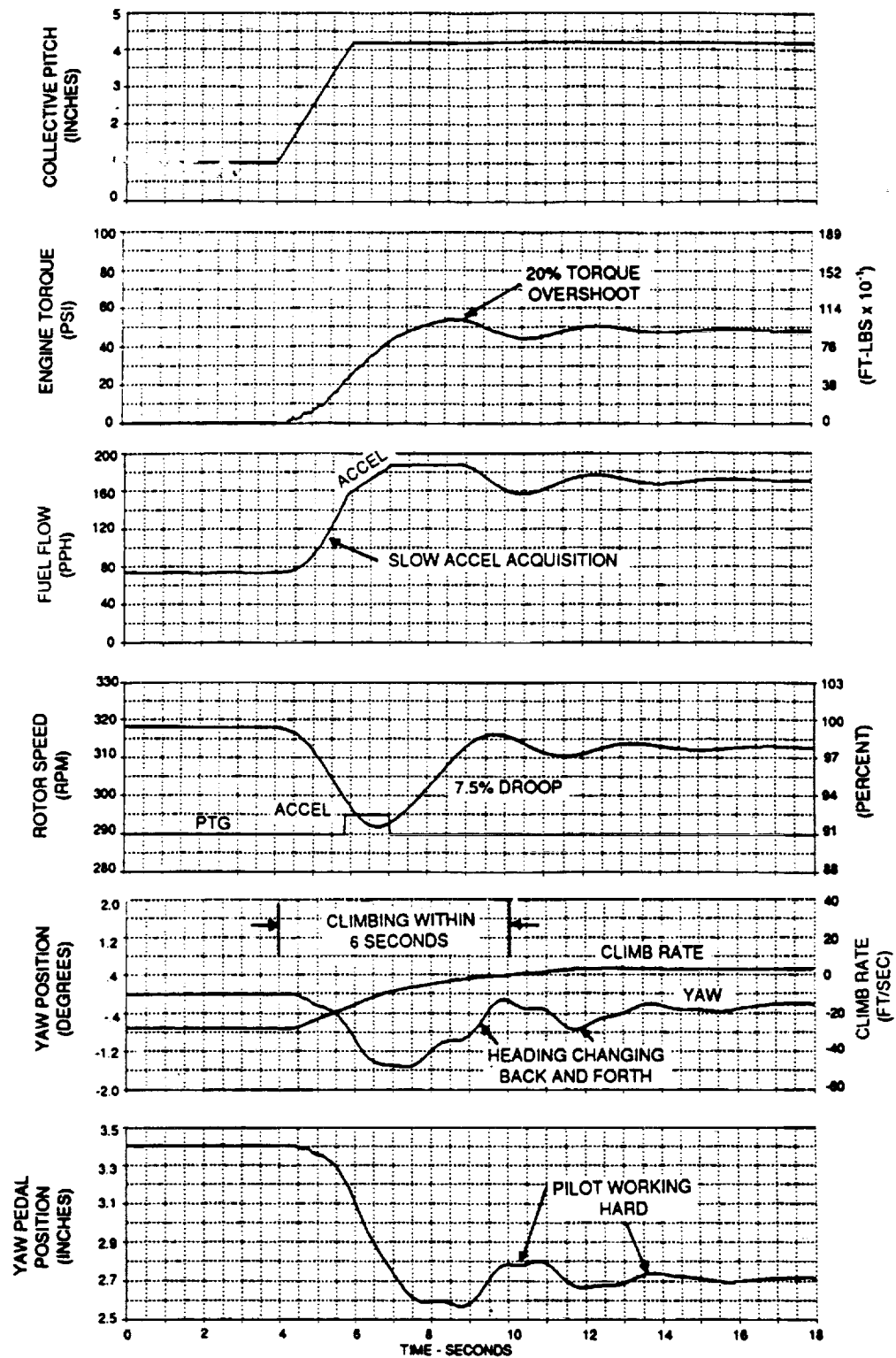


**FREQUENCY RESPONSE COMPARISON OF  
POWER TURBINE SPEED CONTROL - NF/NF  
WIDEBAND GOVERNOR vs. TA CONTROL**



**TORQUE DISTURBANCE REJECTION COMPARISON - NF/QD  
WIDEBAND GOVERNOR vs. TA CONTROL**

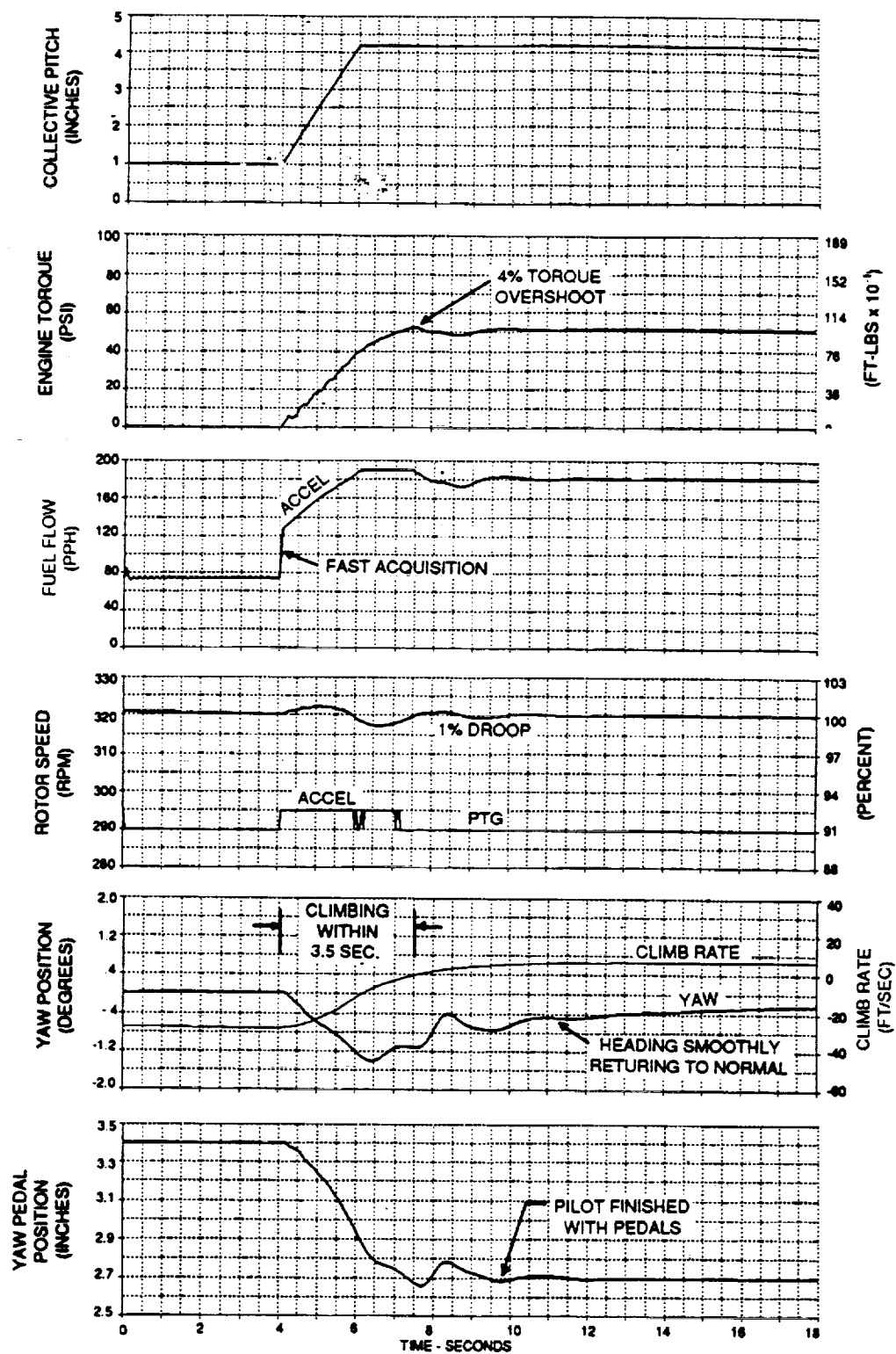
Figure 21



## TA HYDROMECHANICAL PTG PERFORMANCE

2 Second Collective Pull from Low to High Power

Figure 22



**WIDEBAND ELECTRONIC PTG PERFORMANCE**  
**2 Second Collective Pull from Low to High Power**  
 Figure 23



## PRELIMINARY DESIGN...FADEC SYSTEM

The results of the previous section clearly point to an electronic solution of the rocket fire surge problem. Engine fuel flow must be modulated very rapidly using sophisticated control laws in order to kill drive train oscillations before they have a chance to build up.

Therefore, a microprocessor based controller is required in order to incorporate the sophisticated logic in software.

The TA hydromechanical control contains a completely separate fuel metering system for emergency operation. This metering system can be readily interfaced to a FADEC system thereby taking full advantage of the electronic control. A single channel FADEC can be used, thereby limiting the modifications to the aircraft. Electronic sensors can be shared with existing cockpit instruments. And, flight safety is enhanced because the primary hydromechanical TA control remains on board to serve as a backup in case of failure of the electronic control.

### **Electronic Control Unit**

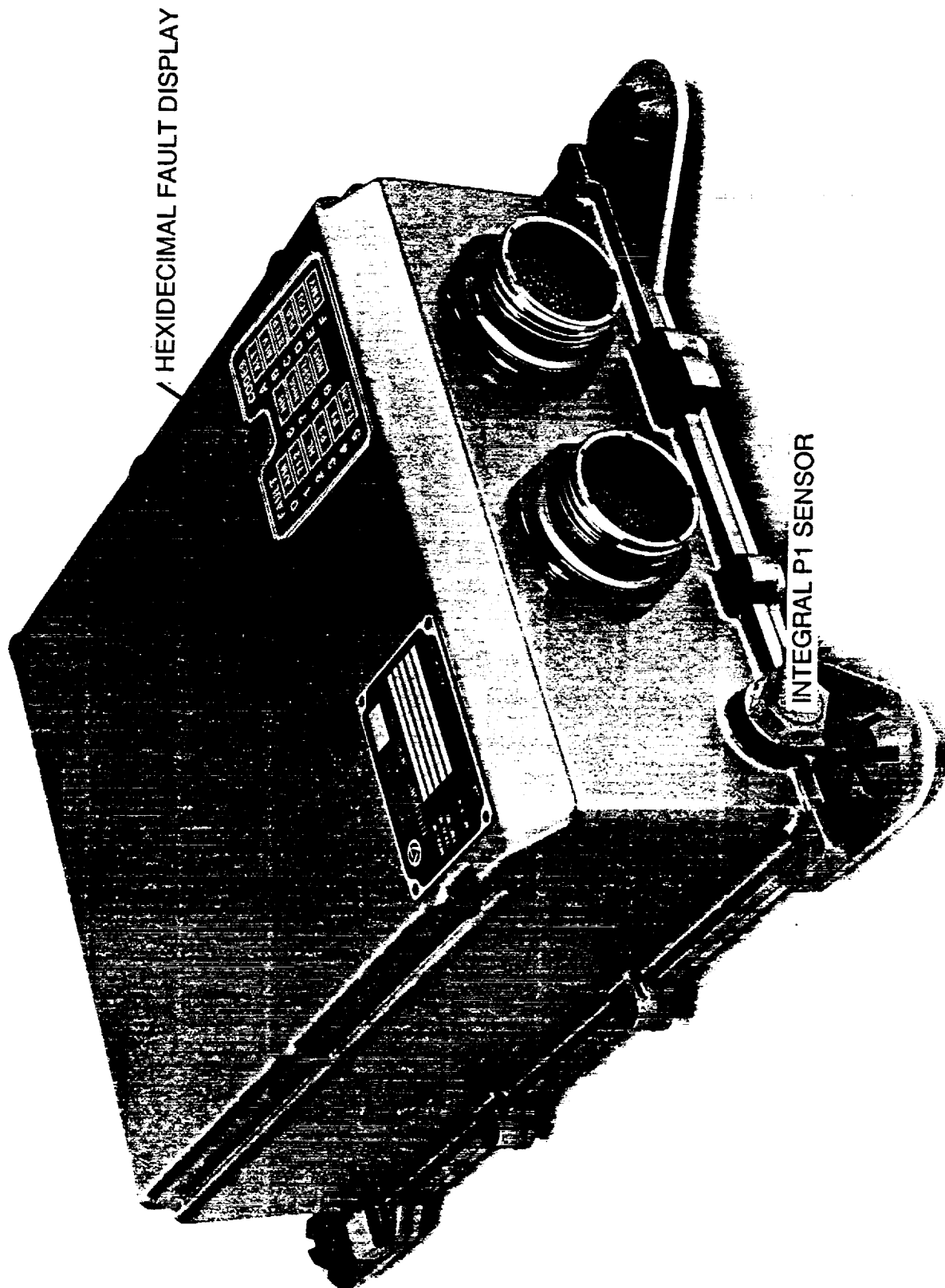
#### Hardware

Chandler Evans is at the present time completing a full-scale development and certification program of a "generic" FADEC which is shown in Figure 24. The generic FADEC was designed from the onset to be adaptable to many applications with minimal design changes. It has considerable computing power, extensive input/output signal processing capability, is modular in design, and has provision for an application board to accommodate the unique requirements of each particular installation.

Existing sensors are utilized where possible and shared with cockpit gages as necessary. Therefore, airframe modifications are minimized. The FADEC is powered from the aircraft's 28V DC bus and requires approximately 100 watts under peak load conditions.

Separate overspeed protection is provided within the FADEC enclosure. An analog overspeed system with an independent power supply operates through the existing engine mounted overspeed solenoid to chop fuel flow to minimum flow on detection of an overspeed condition.

The FADEC I/O lines are extensively shielded and filtered to provide lightning protection and EMI insensitivity to DO 160C, 200 V/M fields. Therefore, the primary control as well as the overspeed system are insensitive to external upsets.



HEXIDECIMAL FAULT DISPLAY

INTEGRAL P1 SENSOR

CHANDLER EVANS "GENERIC" FADEC

Figure 24

## Software

The software architecture is illustrated in Figure 25. Range, rate, and difference tests are applied as well as reasonability tests based on Kalman Filter errors. These errors are the difference between computed states and actual sensor measurements. Only validated signals are passed on to the engine control laws.

The engine and airvehicle control functions provided by the FADEC system are illustrated in Figure 25 and are described below.

### *Wideband Power Turbine Governor*

A high response governor that minimizes transient rotor speed droop and torque overshoots during maneuvering flight and damps out rotor drive train oscillations during rocket fire surge. Isochronous (constant speed) governing is provided in steady state.

### *Gas Generator Governor*

Provides isochronous NG governing as a function of PLA position between ground idle and maximum power.

### *T4.5 Limiter*

Provides gas temperature limiting during starting to preclude hot starts and for engine protection at high power settings.

### *Torque Limiter*

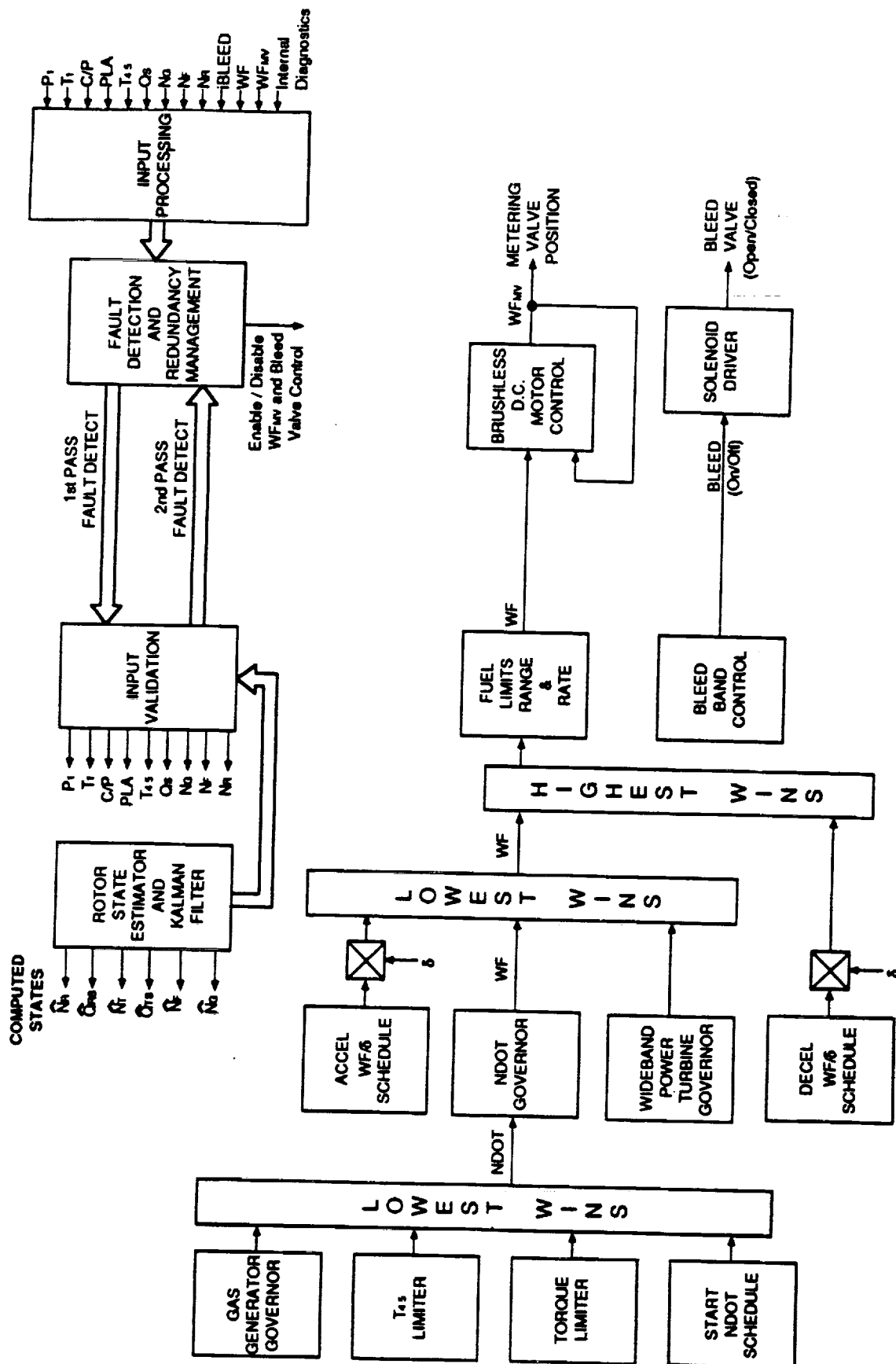
Provides output shaft torque limiting to preclude overstressing the rotor drive train during steady state as well as transient conditions. Allows the pilot to fly the helicopter at or near the torque limit for improved maneuverability.

### *NDOT Schedule*

The start engine control law is based on NDOT, i.e., gas generator acceleration rate. This allows closed loop control of engine starts which is more accurate than the open loop  $Wf/\delta$  control law employed in the hydromechanical TA control. Therefore, repeatable engine starts can be achieved without overtemperaturing the engine. During starting, the engine will achieve idle under varying ambient conditions without hanging because of the closed loop control of acceleration rate, NDOT.

### *Accel $Wf/\delta$ Schedule*

The existing  $Wf/\delta$  open loop acceleration schedules that are implemented in the TA hydromechanical control are retained in the FADEC implementation. The engine has been qualified with these limits, therefore, there is no need to change these schedules. Furthermore, the open loop schedules will be more accurate with the digital electronic implementation, thereby giving more repeatable transient performance.



T53 FADEC . . . SOFTWARE ARCHITECTURE  
Figure 25

#### *Decel Wf/δ Schedule*

The existing Wf/δ open loop deceleration schedules that are implemented in the TA hydromechanical control are also retained in the FADEC for the same reasons as above.

#### *Fuel Limits Range and Rate*

Absolute fuel flow limits and rate limits are imposed on the final Wf demand. These preclude overfueling and flameout and provide further checking of processor functionality before actually positioning the fuel metering valve.

#### *Bleed Band Control*

FADEC control of the pneumatic bleed band actuator is provided via an on/off solenoid valve. The existing logic that is implemented in the TA hydromechanical control will be utilized for the same reasons as above. However, this interface is available to improve surge recovery with additional logic if engine/flight test shows that it is of benefit.

In summary, sophisticated engine and rotor speed control is provided to enhance flight safety (rocket fire torque spikes are eliminated); improve engine performance (repeatable starts, temperature and torque limiting); and enhance helicopter maneuverability and handling qualities (reduced rotor speed droop and torque overshoot with less pilot workload). Furthermore, extensive fault coverage is provided such that if an electronic control or sensor failure should occur, the fuel metering valve fails fixed at its current position. An indication is given to the pilot at which time he or she can transfer to the bill-of-material TA hydromechanical control for a safe continuation of the flight.

#### **TA Control Modifications**

The fuel metering section of the TA hydromechanical control is illustrated in Figure 26. Two separate metering systems consisting of a metering valve and dedicated head regulator are provided. The backup metering valve is positioned by the hydromechanical TA computer consisting of speed, temperature, and pressure servos and 3-D cams (not shown). The primary metering valve is a rotary valve, positioned by an electric motor. A transfer valve and solenoid which is actuated by a cockpit switch determines which metering system is in control of engine fuel flow. The motor and controller are designed to fail-fixed, thereby giving the pilot time to manually transfer to the TA hydromechanical control for safe continuation of flight.



TAT59  
A032013 A

A layout drawing of the DC motor and gearhead interface to the TA control is shown in Figure 27.

The new hardware fits in a module placed between the power turbine governor and the cover for the main hydromechanical computer. The change involves one new casting for the motor module. In addition, the PTG housing cover must be redesigned for mounting purposes. Aside from a slight 0.5 inch movement of the fuel discharge port, the only change affecting installation is the addition of an electrical connector. All other interfaces remain unchanged. Inspection of the actual AH-1 aircraft installation indicates that these hardware changes are feasible within the current space limitations.

### **Engine and Airvehicle Modifications**

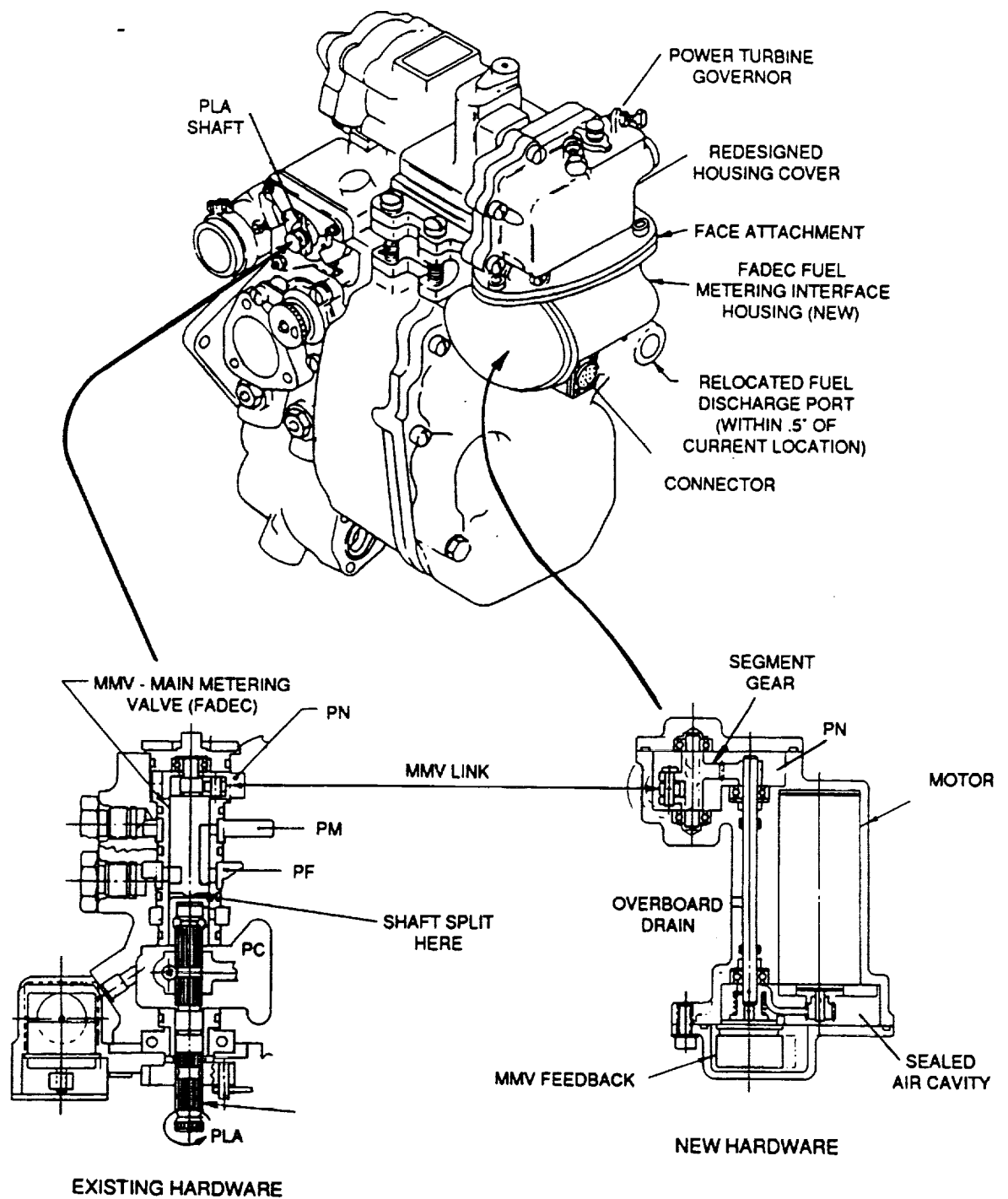
The modifications to the AH-1/TS3 airvehicle for the single channel FADEC system with the existing TA hydromechanical control as backup are summarized below.

#### *Cockpit*

- 1) No additional inputs are required. The existing emergency reversion switch will be used to transfer between FADEC and the TA control. And, the rotor operates at constant, 100% rpm when on the power turbine governor, therefore, a speed set adjustment is not required for electronic control.
- 2) Install a FADEC fault lamp and an overspeed test fault lamp in the cockpit. These give the pilot an indication of FADEC status and the results of the automatic overspeed test which is performed during an engine start. Based on this information, the pilot can abort a flight or transfer to the TA hydromechanical control while in the air to continue the mission.

#### *Engine*

- 1) Install a T1 RTD at the engine inlet.
- 2) Install a gear-up mechanism and a magnetic speed pickup, one for Ng and one for Np between the existing tach generator used for cockpit display and the engine drive pad.
- 3) Install bleed band control and transfer solenoids in the pneumatic line feeding the TA control. The transfer solenoid is activated by the existing emergency reversion switch that is used to transfer between FADEC and the TA control. The bleed band control solenoid is modulated by the FADEC. Both solenoids are wired such that loss of electrical power causes reversion to the TA hydromechanical control.
- 4) Provide an electrical harness for the above engine sensors, the bleed solenoids, the shared QS and T4.5 sensors, and the TA control to the FADEC.



# **MODEL TA-7 CONTROL MODIFIED FOR FADEC INTERFACE**

Figure 27



#### *Airframe*

- 1) Install collective pitch and PLA RVDTs on the linkages between the pilot's stick and the TA control. -
- 2) Provide an electrical harness from the above sensors, the shared rotor speed sensor, and 28V DC power to the airframe mounted FADEC.

As shown above, cockpit and airframe modifications are minor and engine modifications are straightforward. The major cost of the FADEC system is the FADEC unit itself with its electric motor interface to the TA control. It is estimated that the cost of the FADEC hardware (electronic control and modifications to the hydromechanical control) is approximately equal to the cost of a TA hydromechanical control overhaul.

#### CONCLUSIONS AND RECOMMENDATIONS

- 1) The AH-1/T53 Cobra rotor drive train is very lightly damped. Therefore, any significant disturbances such as rocket fire surges or potential fuel control or IGV corrections that are not phased properly tend to excite the torsional modes of the drive train and cause transient overtorques.
- 2) An electronic control, however, modulating engine fuel flow and torque in direct opposition to drive train resonances has been shown by simulation to damp out torque spikes and hold them within normal operating limits. The electronic control can be readily interfaced to the existing TA hydromechanical unit via its separate emergency fuel valve. This controller also provides an inherently faster engine and rotor speed control loop for normal operation. Thus, transient rotor speed droop and engine torque overshoots during aggressive maneuvers are significantly reduced as compared to the existing bill-of-material control. Thus, a side benefit of increased helicopter agility with less pilot workload is realized.
- 3) Because the above work is based on a simulation of the engine, it is recommended that an engine test be performed whereby high frequency fuel flow inputs are applied to the engine. The objectives of this test are to:
  - a) Verify that rapid fuel flow modulation will not adversely affect the T53 engine.

Previous work performed under U.S. Army contract showed that this concept is feasible using the 250 engine (Reference AVSCOM Technical Reports: USAAVRADCOM-TR-83-D-1, Adaptive Fuel Control Feasibility Investigation, dated 1983; USAAVSCOM-TR-86-D-14, Adaptive Electronic Fuel Control for Helicopters...250 Engine Testing and 206L Helicopter Flight Test, dated 1986). Therefore, a high confidence level exists that the rocket fire problem can be solved by modulating fuel flow as described herein.

- b) Verify the engine's fast path fuel flow to torque relationship. Combustive damping of the drive train resonances is highly dependent on this gain. The final control design requires an accurate definition of this path.
- c) Verify the engine's combustor and gas generator small signal response characteristics beyond the tail rotor resonant frequency of approximately 10 Hz. Again, the final control design requires a good definition of the core engine response.

The engine test can be performed with the existing TA control and an off-the-shelf PC based controller operating a high response fuel valve that is switched in at various operating conditions of the engine to modulate Wf about the steady running condition.

- 4) Depending on the success of the above engine test, an AH-1/T53 Cobra flight test demonstration is recommended. A single channel FADEC interfaced to the modified TA control is recommended to insure flight worthy hardware. The objectives of this test are:
  - a) Demonstrate combustive damping of the rotor drive train. Torsionals can be easily induced on the Cobra drive train by modulating PLA.
  - b) Demonstrate enhanced maneuvering capability and handling qualities.
  - c) Demonstrate insensitivity of the system to rocket fires.
- 5) Depending on the success of the flight test demonstration and a life cycle cost study, it is recommended that the FADEC system with TA hydromechanical backup be considered for incorporation into a U.S. Army or National Guard fleet of Cobra helicopters. Or, the advanced control concepts can be incorporated into modern FADEC equipped helicopters such as Comanche.

## **APPENDIX A**

## List of Symbols and Acronyms

AATD	Aviation Applied Technology Directorate (U.S. Army)
ADOT	Helicopter Vertical Velocity
AVSCOM	Aviation Systems Command (U.S. Army)
BEEP	Pilot's Rotor Speed Trim to TA Control
BF	Power (Free) Turbine Damping
BLEED	Engine Bleed Band Position
BR	Main Rotor Damping
BT	Tail Rotor Damping
C/P	Pilot's Collective Pitch Input
CDP	Compressor Discharge Pressure
FADEC	Full Authority Digital Electronic Control
IGV	Engine Inlet Guide Vane Position
JF	Power (Free) Turbine Inertia
JGB	Gear Box Inertia
JR	Main Rotor Inertia
JT	Tail Rotor Inertia
KR	Main Rotor Mast Spring Rate
KS	Engine Output Shaft Spring Rate
KT	Tail Rotor Shaft Spring Rate
NI	Gas Generator Speed Computer Output (TA Control)
NASA	National Aeronautics and Space Administration
NDOT	Gas Generator Acceleration
NF	Power (Free) Turbine Speed
NG	Gas Generator Speed
NGB	Gear Box (Engine to Rotor Drive Train) Speed
NR	Main Rotor Speed
NT	Tail Rotor Speed
PI	Engine Inlet Pressure

PAMB	Ambient Pressure
PB	Boost Pump Pressure (TA Control)
PC	Case Pressure (TA Control)
PEDALS	Pilot's Tail Rotor Pitch Input
PLA	Power Lever Angle (TA Control)
PM	Metering Valve Discharge Pressure (TA Control)
PN	Engine Nozzle Fuel Pressure
PS	Servo Pressure (TA Control)
PTG	Power Turbine Governor
QD	External Torque Disturbance to Rotor Drive Train
QF	Engine Gas Torque
QRS	Main Rotor Mast Torque
QS	Engine Output Shaft Torque
QTS	Tail Rotor Shaft Torque
SHP	Engine Shaft Horsepower
T1	Engine Inlet Temperature
T1SENSE	Lagged T1 Sensor Output (TA Control)
T4.5	Interstage Turbine Temperature
TA	Turbine Assembly
TECOM	Test and Evaluation Command (U.S. Army)
WF	Engine Fuel Flow
WFSS	Engine Steady State Fuel Flow
WFMV	Metering Valve Position (TA Control)
XDOT	Helicopter Forward Velocity
YAW	Helicopter Heading Change
$\delta$	P1/14.7
$\Theta$	$(T1 + 460)/519$
$\tau$	Linearized First Order Time Constant

## List of Figures

- Figure 1     -     AH-1/T53 Engine Control System
- Figure 2             TA Control System...Functional Block Diagram
- Figure 3             T53 Core Engine...Functional Block Diagram
- Figure 4             Rocket Fire Engine Surge Simulation
- Figure 5             AH-1/T53 Rotor Drive Train - Schematic
- Figure 6             AH-1/T53 Rotor Drive Train - Functional Block Diagram
- Figure 7             AH-1/T53 Rotor Drive Train Frequency Response - NF/QF
- Figure 8             Definition of Flight Maneuver ... Gun Run
- Figure 9             Simulated Flight Maneuver ... Gun Run
- Figure 10            MK66 Rocket Fire Flight Test Data (1 Pair)
- Figure 11            Simulation of MK66 Rocket Fire Flight Test (1 Pair)
- Figure 12            Simulation of Multiple Rocket Fires (3 Pair)
- Figure 13            Simulation of Rocket Fire Flight Test (1 Pair)...With Fuel Flow Constant
- Figure 14            Simulation of Multiple (19) Rocket Fires...With IGV Synched to Rocket Fire
- Figure 15            Simulation of Rocket Fire Flight Test (1 Pair)...With IGV Synched to Surge
- Figure 16            Combustive Damping Block Diagram
- Figure 17            Effect of Active Damping on AH-1/T53 Rotor Torsionals Torque Disturbance Rejection NF/QD
- Figure 18            Simulation of Rocket Fire Flight Test (1 Pair)...With Electronic Combustive Damping
- Figure 19            Simulation of Multiple Rocket Fires (3 Pair)...With Electronic Combustive Damping
- Figure 20            Effect of Combustive Damping on AH-1 Rotor Drive Train Torsionals

- Figure 21      Frequency Response Comparison of Power Turbine Speed Control - NF/NF  
Wideband Governor vs. TA Control  
—      Torque Disturbance Rejection Comparison - NF/QD Wideband Governor vs. TA  
Control
- Figure 22      TA Hydromechanical PTG Performance...2 Second Collective Pull from Low  
to High Power
- Figure 23      Wideband Electronic PTG Performance...2 Second Collective Pull from Low to  
High Power
- Figure 24      Chandler Evans "Generic" FADEC
- Figure 25      T53 FADEC...Software Architecture
- Figure 26      Model TA-7 "Modified" Fuel Metering Section...Schematic
- Figure 27      Model TA-7 Control Modified for FADEC Interface...Layout Drawing

REPORT DOCUMENTATION PAGE			Form Approved OMB No. 0704-0188	
Public reporting burden for this collection of information is estimated to average 1 hour per response, including the time for reviewing instructions, searching existing data sources, gathering and maintaining the data needed, and completing and reviewing the collection of information. Send comments regarding this burden estimate or any other aspect of this collection of information, including suggestions for reducing this burden, to Washington Headquarters Services, Directorate for Information Operations and Reports, 1215 Jefferson Davis Highway, Suite 1204, Arlington, VA 22202-4302, and to the Office of Management and Budget, Paperwork Reduction Project (0704-0188), Washington, DC 20503.				
1. AGENCY USE ONLY (Leave blank)	2. REPORT DATE April 1994	3. REPORT TYPE AND DATES COVERED Final Contractor Report		
4. TITLE AND SUBTITLE Hot Gas Ingestion Effects On Fuel Control Surge Recovery and AH-1 Rotor Drive Train Torque Spikes		5. FUNDING NUMBERS  WU- None C-NAS3-26075 1L162211A47		
6. AUTHOR(S)  Frank Tokarski, Mihir Desai, Martin Books, and Raymond Zagranski				
7. PERFORMING ORGANIZATION NAME(S) AND ADDRESS(ES)  Coltec Industries Chandler Evans Control Systems Division West Hartford, Connecticut		8. PERFORMING ORGANIZATION REPORT NUMBER  E-8638		
9. SPONSORING/MONITORING AGENCY NAME(S) AND ADDRESS(ES)  National Aeronautics and Space Administration Lewis Research Center Cleveland, Ohio 44135-3191		10. SPONSORING/MONITORING AGENCY REPORT NUMBER  NASA CR-191047 ARL-CR-13		
11. SUPPLEMENTARY NOTES  Project Manager, George A. Bobula, Vehicle Propulsion Directorate, organization code 0300, NASA Lewis Research Center, (216) 433-3698.				
12a. DISTRIBUTION/AVAILABILITY STATEMENT  Unclassified-Unlimited Subject Category 07			12b. DISTRIBUTION CODE	
13. ABSTRACT (Maximum 200 words)  This report summarizes the work accomplished through computer simulation to understand the impact of the hydro-mechanical turbine assembly (TA) fuel control on rocket gas ingestion induced engine surges on the AH-1 (Cobra) helicopter. These surges excite the lightly damped torsional modes of the Cobra rotor drive train and can cause overtorqueing of the tail rotor shaft. The simulation studies show that the hydromechanical TA control has a negligible effect on drive train resonances because its response is sufficiently attenuated at the resonant frequencies. However, a digital electronic control working through the TA control's separate, emergency fuel metering system has been identified as a solution to the overtorqueing problem. State-of-the-art software within the electronic control can provide active damping of the rotor drive train to eliminate excessive torque spikes due to any disturbances including engine surges and aggressive helicopter maneuvers. Modifications to the existing TA hydromechanical control are relatively minor, and existing engine sensors can be utilized by the electronic control. Therefore, it is concluded that the combination of full authority digital electronic control (FADEC), with hydromechanical backup using the existing TA control enhances flight safety, improves helicopter performance, reduces pilot workload. . .and provides a substantial payback for very little investment.				
14. SUBJECT TERMS  Engine surge; Torque spike; Turbeshaft; Hot gas; Drivetrain oscillation; Active damping; Fuel control			15. NUMBER OF PAGES 54	
			16. PRICE CODE A04	
17. SECURITY CLASSIFICATION OF REPORT Unclassified	18. SECURITY CLASSIFICATION OF THIS PAGE Unclassified	19. SECURITY CLASSIFICATION OF ABSTRACT Unclassified	20. LIMITATION OF ABSTRACT	





**National Aeronautics and  
Space Administration**

**Lewis Research Center**  
21000 Brookpark Rd.  
Cleveland, OH 44135-3191

**Official Business  
Penalty for Private Use \$300**

**POSTMASTER: If Undeliverable — Do Not Return**